AMRO
ASEAN +3 MACROECONOMIC RESEARCH OFFICE

Working Paper (WP/26-04)

Global Banking Default Cycles: Cross-Country Exposure and Business Cycle Implications

Aruhan Rui Shi

June 2026

[This page is intentionally left blank]

Global Banking Default Cycles: Cross-Country Exposure and Business Cycle Implications

Aruhan Rui Shi[†]

June 2026

Abstract

This paper studies a global banking-sector default cycle constructed from firm-level probabilities of default across a broad set of countries and evaluates its macro-financial implications. Using a dynamic factor model, we extract a dominant global component in bank default risk and document substantial cross-country heterogeneity in exposure. We then analyze its association with credit and real economic outcomes. The evidence shows that increases in global banking-sector default risk tend to follow credit tightening and precede declines in real activity, particularly in elevated stress regimes. The relationship is state-dependent, with larger output responses concentrated during stressed periods, while credit dynamics exhibit more persistent adjustment. Overall, the findings indicate that market-implied banking-sector default risk captures periods in which financial strain is reflected in market-based measures of banking stress and is closely linked to real economic weakness.

JEL Classification: C38, E32, E44, F44, G01, G21.

Keywords: banking-sector default risk; default cycles; global financial conditions; macro-financial linkages; dynamic factor models.

[*]Email: aruhanruishi@outlook.com (permanent), aruhan.rui.shi@amro-asia.org. This paper was authorized for distribution by Abdurohman, Deputy Director.

[†]I am especially grateful to Jorge A. Chan-Lau for suggesting this research direction, providing the initial code infrastructure for estimating the DFM, and offering extensive comments, guidance, and helpful discussions throughout the project. I thank Min Wei for valuable assistance with the PD dataset and related analyses. I am also grateful to Sekar U. Setiastuti and Jerry Huang for helpful comments and suggestions. The views expressed are those of the author and do not necessarily represent the views of AMRO. All remaining errors are my own.

1 Introduction

Global financial integration has increased the degree of interconnectedness across national financial systems, contributing to stronger cross-country comovement in financial conditions. Episodes of global financial turmoil repeatedly show that measures of bank default risk rise simultaneously across countries, even in the absence of large domestic shocks. This co-movement suggests that banking-sector distress reflects not only country-specific fundamentals but also exposure to shared global financial conditions. Given the central role of banks in credit intermediation, understanding the nature and implications of these common forces is central to macro-financial surveillance. In particular, while financial cycle indicators capture fluctuations in credit conditions and risk-taking, they do not directly measure realized balance-sheet stress within the banking sector.

Observed synchronization in banking-sector default risk does not necessarily imply direct contagion across banking systems and may instead reflect exposure to common global shocks. While such co-movement is often attributed to financial interconnectedness, disentangling spillovers from common shocks is empirically challenging. An alternative perspective is that an unobserved global factor—reflecting shifts in risk appetite, funding conditions, or expectations—jointly drives banking-sector default risk across countries. Identifying and characterizing such a latent global default cycle is therefore valuable for interpreting observed co-movements in bank risk and for assessing the macro-financial information embedded in market-implied banking stress, as emphasized in Chan-Lau (2026).

This perspective relates to broader strands of the literature documenting common global cycles in financial conditions. Studies such as Miranda-Agrippino and Rey (2020) show that global risk appetite and financial conditions co-move strongly across countries and shape domestic macro-financial outcomes. Our approach complements this work by examining a banking-sector–specific manifestation of global financial risk, extracted from market-implied default probabilities rather than asset prices. In addition, the analysis is conceptually related to models of correlated default and frailty (Duffie et al., 2009), which emphasize the role of unobserved common factors in driving joint default risk.

A wide range of theoretical frameworks imply a connection between banking-sector stress and macro-financial outcomes, including models emphasizing balance sheet constraints (Kiyotaki and Moore, 1997; Bernanke et al., 1999), risk-taking behavior, and shifts in expectations or global financial conditions (Shin, 2013; Adrian and Shin, 2010). These theories provide motivation for examining the macro-financial relevance of banking-sector default risk.

Against this background, this paper revisits the notion of a global banking-sector default cycle and examines its macro-financial relevance using updated data and a complementary empirical perspective. Building on Chan-Lau (2026), we extend the analysis using a longer and more recent panel of market-based probabilities of default for banking-sector firms across a broad set of economies. Applying a dynamic factor model, we extract latent components that capture shared movements in bank default

risk and focus on the economic interpretation of the dominant global factor. Rather than modeling the determinants of default behavior, this paper evaluates the macro-financial associations of global banking-sector default risk.

The paper makes three contributions. First, using panel local projections, we find that global banking-sector default risk has economically meaningful predictive content for macro-financial outcomes: a one-standard-deviation increase in the global banking stress factor is followed by a decline in GDP growth of approximately 1.27 percentage points at a one-quarter horizon and a persistent widening of the credit-to-GDP gap reaching nearly one percentage point by one year ahead. We also find suggestive evidence that these associations strengthen during periods of elevated stress, though the results are sensitive to the choice of stress threshold. Second, we document that cross-country exposure to the global cycle is highly heterogeneous: while most banking systems load positively on the global factor, the strength of this loading varies considerably across regions, with Asian economies exhibiting more dispersion than their Western counterparts. Third, building on Chan-Lau (2026), we extend the analysis to a longer and more recent panel, confirming that the estimated global factor continues to align with major episodes of financial stress—the global financial crisis, the European sovereign debt crisis, and the COVID-19 shock.

While the analysis is reduced-form and does not identify structural transmission mechanisms, the findings collectively support treating market-implied banking-sector default risk as a forward-looking complement to conventional surveillance indicators—one whose informational content is most pronounced precisely when financial conditions deteriorate most severely.

The remainder of the paper is organized as follows. Section 2 reviews the related literature. Section 3 outlines the empirical framework. Section 4 describes the data. Section 5 presents the dynamic factor model results and characterizes cross-country and regional heterogeneity in exposure to the global banking-sector default factor. Section 6 examines the macro-financial linkages between the global default factor and macro-financial outcomes, namely real GDP growth and the credit-to-GDP gap. Section 7 concludes.

2 Related literature

This paper relates to three strands of the literature on default risk, global financial conditions, and macro-financial linkages.

First, this paper builds on the literature that studies default risk as a systematic phenomenon driven by latent common components. A central insight of this literature is that default risk exhibits persistent time variation and cross-sectional comovement that are not fully spanned by observable macroeconomic variables, credit quantities, or asset prices. Early work using state-space and latent-factor

models demonstrates that credit risk and default intensities contain systematic components that evolve over time and reflect shifts in underlying economic and financial conditions (e.g., Koopman and Lucas (2005)). Subsequent contributions emphasize that default dynamics are related to, but distinct from, business and credit cycles, and therefore warrant separate measurement and analysis.

More recent work explicitly conceptualizes and measures default cycles as recurring fluctuations in default risk over time. In particular, Chan-Lau (2026) exploit firm-level probabilities of default within a dynamic factor model framework to extract common default cycles and to study their dynamics and interactions across sectors. Complementary work in the credit risk modeling literature highlights that default clustering across firms can arise from unobserved common factors, as formalized in frailty and correlated default models (Duffie et al., 2009). Together, these studies underscore that observed co-movement in default risk may reflect exposure to shared latent shocks rather than direct contagion or purely idiosyncratic events. While this literature primarily focuses on identifying and characterizing default dynamics themselves, the present paper takes the global banking-sector default cycle as given and treats it as an informational object, examining its cross-country exposure and macro-financial relevance rather than its internal propagation mechanisms.

Second, the analysis relates to the macro-finance literature on global financial conditions and their implications for real economic activity. A central insight of this literature is that a substantial share of international comovement in financial variables can be traced to a small number of global factors associated with shifts in risk appetite, funding conditions, and intermediary balance sheets. Influential contributions by Rey (2015) and Miranda-Agrippino and Rey (2020) document the existence, strength, and evolution of a global financial cycle reflected in asset prices, capital flows, and leverage conditions. In this environment, banking-sector default risk can be viewed as a downstream manifestation of global financial conditions, capturing how common shifts in risk and funding translate into changes in perceived bank solvency.

A large body of macro-finance research further shows that forward-looking financial indicators such as credit spreads and risk premia contain substantial predictive information about future business-cycle fluctuations (Gilchrist and Zakrajšek, 2012; López-Salido et al., 2017). While this paper does not seek to identify or measure the global financial cycle per se, it complements this literature by examining a closely related but distinct object: a banking-sector–specific global default factor extracted from market-implied probabilities of default rather than from asset prices, and by assessing whether this default-based measure contains forward-looking information about aggregate credit and real economic outcomes.

Finally, the paper builds on methodological advances that use data-rich environments to study latent common factors and dynamic macro-financial relationships in a flexible and robust manner. Dynamic factor models provide a natural framework for extracting shared components from large panels of financial time series and have been widely used to summarize systemic risk and global conditions (Stock and Watson, 2002). Local projections, introduced by Jordà (2005), allow for the estimation of dynamic

responses without imposing strong restrictions on the underlying data-generating process. Combining these approaches, we use a dynamic factor model to identify a global banking-sector default factor and local projections to examine its macro-financial relevance in a reduced-form setting, without seeking to identify structural transmission mechanisms or to discriminate among competing theoretical models.

3 Empirical strategy

This section outlines the empirical framework used to measure global and country-level banking stress and to assess its macro-financial linkages. The strategy proceeds in three steps. First, we extract latent common factors from firm-level banking-sector default risk using a dynamic factor model. Second, we construct country-level banking stress indices and characterize their synchronization with the global factor and within regions. Third, we estimate panel local projections to quantify the dynamic and state-dependent associations between global banking stress and real activity and credit conditions.

3.1 Dynamic factor model of banking-sector default risk

To extract common movements in banking-sector default risk, we estimate a dynamic factor model (DFM) on a panel of market-implied probabilities of default for banking-sector firms. The DFM decomposes observed firm-level default risk into a small number of latent common factors and idiosyncratic components, allowing for heterogeneous factor loadings across firms and countries.

Dynamic factor models provide a flexible framework for summarizing comovement in high-dimensional datasets, particularly in settings where the number of observed time series is large relative to the length of the time dimension. Originally introduced to capture comovements in economic time series (Geweke, 1977), DFMs have become a standard tool in macroeconomic and financial analysis. A large body of empirical work shows that a small number of latent factors can account for a substantial fraction of the variation in macroeconomic and financial variables (Stock and Watson, 2011; Bai and Ng, 2008).

In a DFM, the comovement among a large cross section of observed variables is driven by a small set of unobserved dynamic factors, while each series is also affected by an idiosyncratic component that captures measurement error and firm-specific dynamics not explained by the common factors. The latent factors are treated as summary indices of common conditions rather than structural shocks and evolve over time according to a stochastic process, typically specified as a vector autoregression. Accordingly, the extracted factors should be interpreted as reduced-form measures of common macro-financial conditions rather than as structural primitives. Cross-country differences in institutional characteristics—such as regulatory frameworks or supervisory quality—are not explicitly modeled, but may instead be reflected indirectly in heterogeneous factor loadings and country-level exposure to the global factor. This reduced-form representation is therefore well suited to extracting a global compo-

nent in banking-sector default risk without imposing strong assumptions on the underlying transmission mechanisms.

Formally, let $x_{i,t}$ denote the observed default-risk measure for banking-sector firm i at time t, where t is measured at the monthly frequency. The dynamic factor model decomposes $x_{i,t}$ into a systematic component driven by a small number of latent common factors and an idiosyncratic component:

$$x_{i,t} = \lambda_i' f_t + e_{i,t}, \tag{1}$$

where f_t is a $K \times 1$ vector of latent common factors, λ_i is a firm-specific vector of factor loadings, and $e_{i,t}$ is an idiosyncratic error term capturing firm-level shocks and measurement noise.

The latent factors evolve according to a vector autoregressive process:

$$f_t = \sum_{j=1}^{p} A_j f_{t-j} + u_t, \tag{2}$$

where A_j are coefficient matrices governing factor dynamics and u_t is a vector of innovations.

Idiosyncratic components follow weakly dependent processes:

$$e_{i,t} = \sum_{l=1}^{q} \phi_{i,l} e_{i,t-l} + \eta_{i,t}, \tag{3}$$

where $\eta_{i,t}$ is a mean-zero disturbance term that is assumed to be cross-sectionally weakly correlated.

A variety of methods have been developed to estimate latent factors in dynamic factor models. These range from parametric, low-dimensional approaches designed for panels with small cross-sectional dimension, estimated in the time domain using Gaussian maximum likelihood and the Kalman filter (e.g., Stock and Watson, 1989; Sargent, 1989; Quah and Sargent, 1993), to nonparametric methods tailored to large cross sections that rely on cross-sectional averaging techniques such as principal components analysis (Chamberlain and Rothschild, 1983; Stock and Watson, 2002). Moreover, in a hybrid class of estimators that combines the strengths of both approaches, factors are first estimated using consistent nonparametric methods and subsequently used to estimate the parameters of a state-space representation via parametric techniques (Doz et al., 2012; Giannone et al., 2004). This latter approach forms the basis of the factor estimation procedure employed in this paper.[1]

The number of common factors and their dynamic specification are selected using data-driven proce-

[1] Results are robust to the choice of estimation method: re-estimating using the Doz–Giannone–Reichlin two-step procedure yields a global factor with dynamics nearly identical to the baseline Banbura–Modugno EM estimator.

dures standard in the large-N, moderate-T dynamic factor model literature. The number of factors is determined using information criteria for approximate factor models, which are designed to consistently estimate the dimension of the factor space under conditions of factor pervasiveness and weak cross-sectional dependence in the idiosyncratic components (Bai and Ng, 2002). This selection is complemented by a variance-explanation criterion based on the eigenvalues of the sample covariance matrix, ensuring that the retained factors capture the dominant sources of common variation in the data. To mitigate overfitting in finite samples, the final number of factors is chosen conservatively as the minimum of the information-criterion recommendation and the smallest number of principal components required to exceed a pre-specified cumulative variance threshold.

Conditional on the selected factor dimension, the latent factor process is modeled as a finite-order vector autoregression, with the lag length selected using standard multivariate information criteria applied to the principal-component factor estimates. This two-step approach—static factor extraction followed by parametric modeling of factor dynamics—follows established practice in quasi-maximum likelihood estimation of dynamic factor models and has been shown to deliver consistent factor estimates even under limited misspecification (Stock and Watson, 2002; Doz et al., 2012).

3.2 Country-level banking stress indices

We construct country-level banking stress indices to examine the degree of synchronization and comovement across economies and regions with the global banking default factor. Rather than using raw firm-level default probabilities, we construct country-level default indices from the imputed series produced by the dynamic factor model. These imputed series represent Kalman-smoothed, model-consistent estimates of default risk that reduce firm-specific noise and coherently handle missing observations. As a result, the resulting indices provide a more stable and comparable measure of underlying default conditions across countries and over time.

Let $x_{i,t}$ denote the observed default-risk measure for banking-sector firm i at time t. As described above, we estimate a dynamic factor model of the form

$$x_{i,t} = \lambda_i' f_t + e_{i,t}, \tag{4}$$

where f_t is a vector of latent common factors and $e_{i,t}$ captures idiosyncratic firm-level shocks and measurement noise.

The model is estimated in state-space form, which allows missing observations to be imputed and high-frequency noise to be filtered. From the estimated model, we obtain a smoothed (or imputed) series for firm-level default risk, denoted $\tilde{x}_{i,t}$, which corresponds to the conditional expectation of $x_{i,t}$ given the full information set implied by the model.

To construct a country-level measure of banking-sector stress, we aggregate the DFM-imputed firm-level series across banks within each country and period. Specifically, letting $\mathcal{I}_{c,q}$ denote the set of banking-sector firms operating in country c during quarter q, we define

$$D_{c,q} \equiv \frac{1}{N_{c,q}} \sum_{i \in \mathcal{I}_{c,q}} \tilde{x}_{i,q}, \tag{5}$$

where $N_{c,q}$ is the number of firms in $\mathcal{I}_{c,q}$ and $\tilde{x}_{i,q}$ denotes the quarterly aggregation of the monthly imputed series. Quarterly values are constructed as the simple average of monthly observations within each quarter.

This construction yields a country-level banking stress index that reflects both common movements captured by the latent factors and smoothed firm-level variation, while mitigating the impact of missing observations and measurement noise. The resulting index provides a consistent and comparable measure of banking-sector stress across countries and over time.

Synchronization with the global banking stress factor. Let G_q denote the global banking default factor aggregated to quarterly frequency. To assess the extent to which country-level banking stress co-moves with global conditions, we compute rolling-window correlations between $D_{c,q}$ and G_q:

$$\rho_{c,q}^{(W)} \equiv \mathsf{corr}(D_{c,\tau},\, G_\tau)_{\tau=q-W+1}^{q}\,. \tag{6}$$

We summarize these correlations at the regional level by averaging $\rho_{c,q}^{(W)}$ across countries within each region.

Within-region co-movement: raw and net of the global factor. To distinguish regional synchronization driven by global forces from within-region dynamics, we net out the global component of country-level banking stress. Specifically, we estimate country-specific exposures to the global factor:

$$D_{c,q} = \alpha_c + \beta_c G_q + u_{c,q}, \tag{7}$$

and construct a net-of-global series as

$$D_{c,q}^{\mathsf{net}} \equiv D_{c,q} - \hat{\beta}_c G_q. \tag{8}$$

Within each region r containing N_r countries, we then compute average pairwise correlations using

both the raw and net-of-global series:

$$\overline{\rho}_r^{\text{raw}} \equiv \frac{2}{N_r(N_r-1)} \sum_{c<c' \in r} \text{corr}\big(D_{c,q},\, D_{c',q}\big)\,, \tag{9}$$

$$\overline{\rho}_r^{\text{net}} \equiv \frac{2}{N_r(N_r-1)} \sum_{c<c' \in r} \text{corr}\big(D_{c,q}^{\text{net}},\, D_{c',q}^{\text{net}}\big)\,. \tag{10}$$

The difference between these measures captures the extent to which regional banking stress synchronization is attributable to shared exposure to the global banking default cycle.

3.3 Macro-financial linkages: panel local projections

To assess the dynamic relationship between the global banking default factor and macro-financial variables, we employ the local projection method proposed by Jordà (2005). Local projections are well suited to this setting as they allow the impulse response of each variable to be estimated directly at each horizon without imposing the full dynamic structure required by vector autoregressions. This flexibility is particularly important in a macro-financial and cross-country context, where dynamic responses may be heterogeneous, nonlinear, and subject to structural change. Moreover, local projections are robust to misspecification of the underlying data-generating process, with potential misspecification affecting efficiency rather than consistency, making them attractive in environments characterized by complex dynamics and estimated shock measures (Jordà et al., 2024) and (Montiel Olea et al., 2024). Finally, the local projection framework facilitates the inclusion of external regressors and state-dependent specifications, allowing us to examine how macro-financial responses to global default risk vary across stress regimes in a transparent and interpretable manner.

The baseline specification takes the form:

$$y_{c,t+h} = \alpha_c + \beta_h G_t + \varepsilon_{c,t+h}, \tag{11}$$

where $y_{c,t+h}$ denotes the outcome variable (e.g., GDP growth or the credit-to-GDP gap) for country c at horizon h, G_t is the global banking default factor, and α_c denotes country fixed effects. Estimation is conducted for horizons $h = 0, \ldots, H$ to trace out dynamic responses. Time fixed effects are not included, as the global factor is common across countries and would be absorbed by aggregate time effects. Identification therefore relies on time variation in the global factor.

To allow for nonlinear state dependence, we extend the baseline specification to a state-dependent

framework in which responses differ between periods of elevated and normal global banking stress:

$$y_{c,t+h} = \alpha_c + \beta_h G_t + \delta_h \left(G_t \times \mathbb{1}\{G_t > \tau\}\right) + \Gamma_h X_{c,t} + \varepsilon_{c,t+h}. \tag{12}$$

Here, $\mathbb{1}\{G_t > \tau\}$ is an indicator for periods in which the global banking default factor exceeds a common threshold τ, and $X_{c,t}$ includes lagged controls. In this specification, β_h captures the response in low-stress periods, while δ_h measures the incremental response during high-stress periods. The total response in high-stress regimes is given by $\beta_h + \delta_h$.

We define stress regimes using a common threshold on the global banking default factor. Specifically, the high-stress regime is defined as periods in which the global factor exceeds its 90th percentile over the sample. This choice isolates episodes of unusually elevated global banking stress while retaining sufficient observations for inference in the local projection framework.[2]

Inference in the state-dependent setting focuses on the total high-stress response. Accordingly, we conduct Wald tests of the null hypothesis

$$H_0 : \ \beta_h + \delta_h = 0, \tag{13}$$

which directly assesses whether global banking stress has statistically meaningful macro-financial effects during periods of elevated stress.

4 Data

We source firm-level probabilities of default (PDs) from the Credit Research Initiative (CRI) database at the National University of Singapore (CRI, 2023). The sample covers publicly listed firms across multiple sectors and a broad set of countries. These PDs are constructed using the forward intensity modeling framework developed by Duan et al. (2012) and Duan and Fulop (2013). The CRI PDs are model-implied, forward-looking measures of default risk derived within a structural credit risk framework. Specifically, the estimates combine equity market information—such as stock prices and volatility—with firm balance-sheet data to infer default probabilities over a 12-month horizon.

The PD series are available at a monthly frequency and are used at the monthly level when estimating the dynamic factor model. Prior to factor extraction, we restrict the sample to firms classified under the banking sector (sector code 1410). While focusing on listed banking-sector firms improves comparability, heterogeneity within the sector—such as differences in size, ownership, and regulatory environ-

[2]Results are qualitatively robust to alternative threshold definitions. The direction and shape of responses are consistent across the 85th, 90th, and 95th percentile thresholds. For the credit-to-GDP gap, peak-horizon magnitudes tend to increase with the percentile cutoff, consistent with larger effects during more extreme stress episodes. For GDP growth, the 85th percentile yields stronger statistical precision due to the larger high-stress sample, while the 95th percentile produces wider confidence intervals given fewer qualifying observations. See Appendix E for full results.

ment—may still affect default risk and is not explicitly modeled. We further apply a set of data-quality filters designed to mitigate the influence of missing observations while preserving sufficient time-series and cross-sectional variation.

Missing observations arise both across firms and over time. To ensure adequate coverage along both dimensions, we apply a two-step filtering procedure. First, we retain firms whose PD series are sufficiently dense, requiring that at least 80 percent of monthly observations are available over the full sample period. Second, conditional on this firm-selected panel, we drop months in which the cross-sectional share of missing observations exceeds 30 percent. This firm-first ordering is chosen to preserve the historical time span of the sample. Applying the date screen first would eliminate most months prior to 2016 due to sparse early-period coverage in the CRI database, which would remove the Asian financial crisis, the global financial crisis of 2008–09, and the European sovereign debt crisis—episodes that are central to the paper's analysis.[3] The resulting dataset comprises 1,930 firms across 92 economies. The 80 percent data density requirement may introduce sample bias; however, the direction of this bias is ambiguous. Excluding firms with sparse observations disproportionately removes smaller or more distressed entities, which could understate stress during crisis periods. Conversely, the surviving sample is concentrated among larger, more financially integrated institutions, which may exhibit stronger co-movement with global conditions during stress episodes and could overstate the measured degree of systemic stress.

Coverage is strongest among advanced economies in the Americas and Europe, reflecting the broader availability of market-based PD data in these regions. Within ASEAN+3, the sample includes approximately 341 firms from the Plus-3 economies and 181 firms from ASEAN economies.

Table 1: Summary statistics: PD

Region	Mean	Standard deviation	Median	Minimum	Maximum	Number of firms
ASEAN	0.0049	0.0160	0.0019	0.0000	0.5534	181
plus3	0.0080	0.0147	0.0034	0.0000	0.3808	341
Other Asia & Pacific	0.0068	0.0121	0.0028	0.0000	0.2235	400
Europe	0.0033	0.0063	0.0015	0.0000	0.3799	303
Americas	0.0032	0.0101	0.0008	0.0000	0.5770	444
Africa	0.0064	0.0100	0.0031	0.0000	0.2709	60
MENA	0.0041	0.0081	0.0016	0.0000	0.2035	201

Source: CRI and Authors' calculations.

Notes: Summary statistics are computed using firm-level PD observations aggregated by region with filtering. ASEAN denotes the Association of Southeast Asian Nations. *plus3* refers to China, Japan, and Korea. MENA denotes Middle East, North Africa, Afghanistan, and Pakistan.

[3]Over the common post-2016 window, the global banking default factors extracted under the two filtering orders correlate at 0.97, confirming that they capture the same dynamics where the samples overlap.

In addition to firm-level default probabilities, the analysis incorporates measures of global financial conditions and domestic macro-financial outcomes. Global risk sentiment is proxied by the Chicago Board Options Exchange (CBOE) Volatility Index (VIX), sourced from Haver and available at daily frequency. Real GDP data are obtained from the International Monetary Fund (IMF) National Economic Accounts (NEA) database at quarterly frequency covering from 1950 Q1 to 2025 Q3. Credit conditions are captured using the credit-to-GDP gap, sourced from the Bank for International Settlements (BIS) and available at quarterly frequency covering 1995 Q2 - 2025 Q2.

For the macro-financial linkages analysis, all variables are aggregated or transformed to a common quarterly frequency prior to estimation. Real GDP growth is computed on a year-on-year basis. When seasonally adjusted GDP series are available, these are used; otherwise, non-seasonally adjusted series are employed. Because growth rates are measured on a year-on-year basis, residual seasonality is unlikely to materially affect the results. Summary statistics (Table 2 and 3) are computed using the merged BIS–IMF dataset and therefore reflect the effective estimation sample common to all macroeconomic variables.

Coverage is highest among advanced economies in Europe and the Americas, followed by economies in the Asia–Pacific region. Average real GDP growth over the entire sample period is strongest in ASEAN economies, at approximately 4.3 percent, followed by MENA and Plus-3 economies, at 3.8 percent and 3.1 percent, respectively (Table 2). With respect to credit conditions (Table 3), we retain all available credit-to-GDP gap observations in order to maximize country coverage, including economies with unusually large credit gaps—often exceeding 300 percent—which primarily reflect the presence of offshore financial centers and large cross-border financial sectors rather than domestic credit booms.

Table 2: Summary statistics: real GDP growth, in percent

Region	Mean	Standard deviation	Median	Minimum	Maximum	Number of observations	Number of countries
ASEAN	4.3	3.9	4.8	-16.9	18.4	344	4
plus3	3.1	3.6	2.9	-9.5	20.5	298	4
Other Asia & Pacific	4.1	3.4	3.7	-22.0	23.1	357	3
Europe	2.3	4.0	2.2	-21.7	44.9	2548	22
Americas	2.6	3.9	2.6	-20.5	22.5	754	7
Africa	2.3	3.1	2.3	-16.8	19.2	122	1
MENA	3.8	3.6	3.9	-8.0	16.3	176	2

Source: IMF and Authors' calculations.

Notes: The table reports summary statistics for real GDP growth at the quarterly frequency. ASEAN denotes the Association of Southeast Asian Nations. *plus3* refers to China, Japan, and Korea. MENA denotes Middle East, North Africa, Afghanistan, and Pakistan.

Table 3: Summary statistics: credit-to-GDP gap, in percent

Region	Mean	Standard deviation	Median	Minimum	Maximum	Number of observations	Number of countries
ASEAN	138.6	58.7	156.9	25.3	223.4	488	4
plus3	179.1	58.9	170.9	80.0	389.3	485	4
Other Asia & Pacific	141.3	47.9	144.8	55.0	203.2	366	3
Europe	162.4	81.6	150.4	18.5	490.5	2539	22
Americas	92.8	60.5	74.2	20.1	232.7	763	7
Africa	68.9	9.7	73.4	53.1	79.7	122	1
MENA	86.6	37.0	110.4	34.3	130.8	189	2

Source: BIS and Authors' calculations.

Notes: The table reports summary statistics for the credit-to-GDP gap at the quarterly frequency. The credit gap is defined as the deviation of the credit-to-GDP ratio from its long-run trend. ASEAN denotes the Association of Southeast Asian Nations. *plus3* refers to China, Japan, and Korea. MENA denotes Middle East, North Africa, Afghanistan, and Pakistan.

For each country, we aggregate the monthly estimated global banking sector stress factor and the country-level banking stress index, and merge with the macro-financial panel comprising real activity and credit variables.

5 Global banking default cycle: cross-country exposure and synchronization

This section first presents the results from the DFM estimation, which identifies a dominant global banking-sector default factor and summarizes country exposure through time-invariant factor loadings. While these loadings capture average exposure over the sample, they do not allow for time variation or for differences in realized co-movement across country groups. Given the slow-moving and state-dependent nature of financial stress, it is natural to expect that exposure to the global default cycle may vary over time and across regions. We therefore complement the DFM results with a descriptive analysis of time-varying co-movement between country-level default risk and the global factor, highlighting patterns of synchronization and heterogeneity without attempting to explain their underlying drivers[4].

[4]Explaining the sources of time variation and cross-country heterogeneity in exposure to the global default cycle would require a different modeling framework and lies beyond the scope of this paper.

5.1 Global banking default cycle

Factor 1 displays the largest amplitude and most persistent fluctuations over time, with pronounced spikes during well-known episodes of global stress. This is particularly true during the 2020 COVID episode. Its dynamics are characterized by broad-based movements rather than short-lived shocks, suggesting it is likely to be a global factor. Figure 1 reports the five latent factors extracted from the dynamic factor model (Panel A), together with their pairwise correlations (Panel B). The factors exhibit distinct time-series properties and limited contemporaneous correlation, suggesting that they capture different dimensions of variation in bank default risk.

Factor 2 to 5 account for residual variation in default risk and likely represent noise, measurement error, or highly localized dynamics.[5] Factor 2 shows episodic but more localized surges, with notable peaks concentrated in specific periods. Its correlation with Factor 1 is close to zero, indicating that it captures variation largely orthogonal to the global cycle. The moderate positive correlation with Factor 3 suggests that both factors may reflect related, but more transitory, sources of stress—potentially associated with sectoral or regional disturbances rather than global systemic conditions. Factor 3 exhibits higher-frequency fluctuations with relatively limited persistence. While it is moderately correlated with Factor 2, its weak association with Factor 1 indicates that it does not reflect global default dynamics. Instead, it appears to capture short-run or idiosyncratic components of bank default risk that are not synchronized across countries. Factors 4 and 5 are characterized by low volatility and limited persistence, with correlations close to zero with the dominant global factor and with each other.

[5] See Appendix B for summary statistics of factors estimated.

Figure 1: **Extracted Banking-Sector Default Risk Factors**

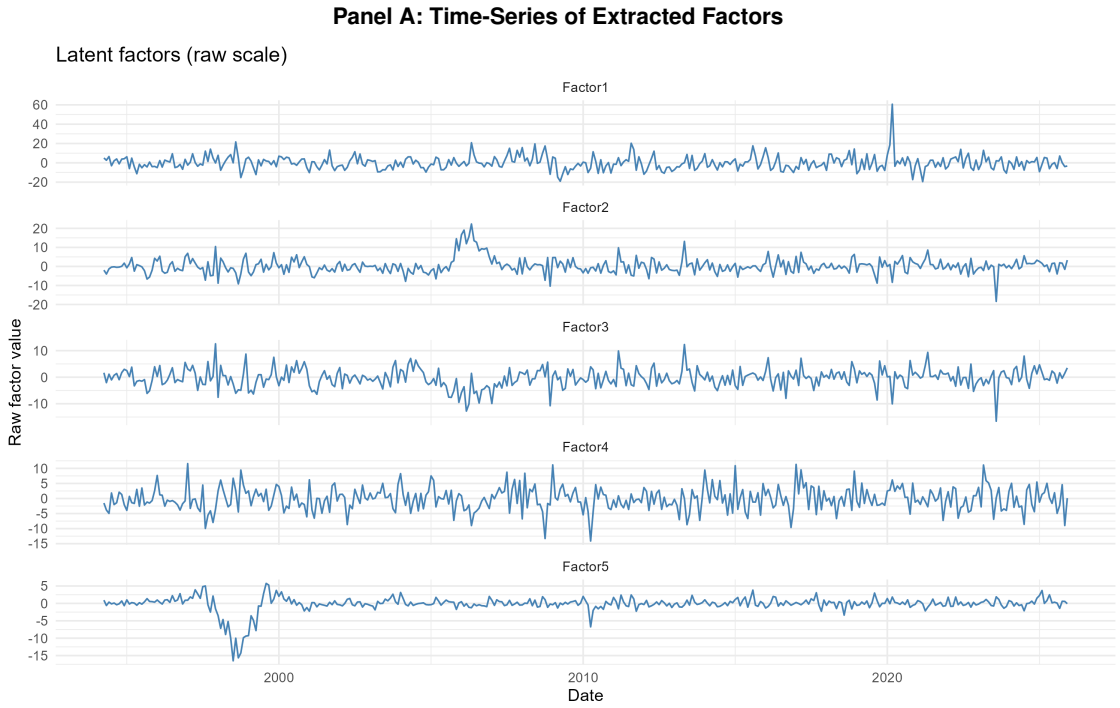

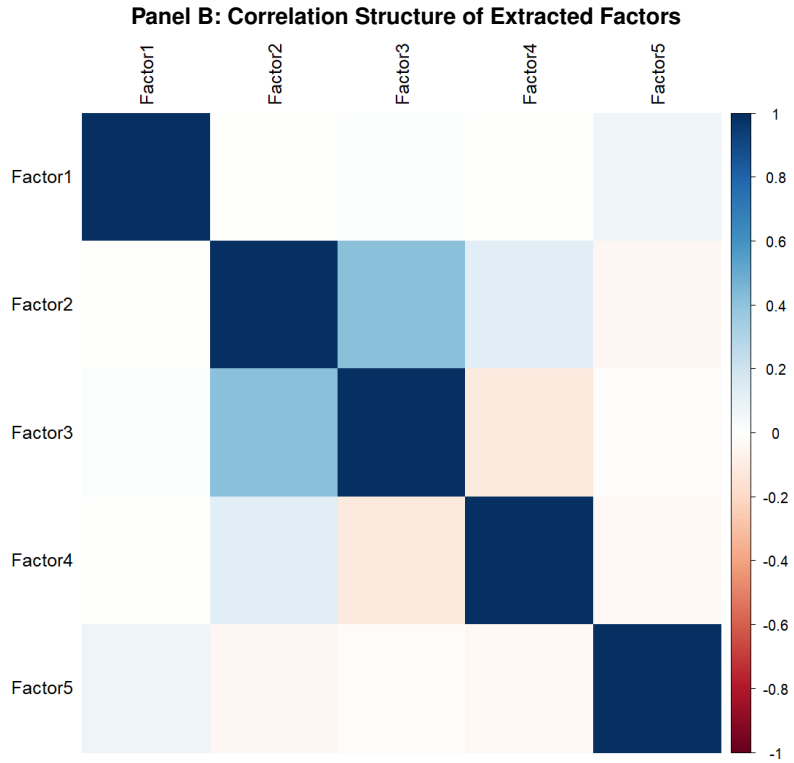

Source: Authors' estimation

Figure 2 and 3 provide further evidence supporting the interpretation of Factor 1 as a global banking default cycle. Figure 2 reports the distribution of factor loadings across banks for each of the five extracted factors. The loading distribution for Factor 1 is markedly different from those of higher-order factors: loadings are predominantly positive and tightly clustered, indicating that a large share of banks across countries load in the same direction on this factor. This contrasts with Factors 2 through 5, whose loading distributions are more dispersed and centered closer to zero, consistent with more localized or idiosyncratic sources of variation. Figure 3 plots Factor 1 together with the cross-country average of bank-level probabilities of default. The two series exhibit strong co-movement over time, with synchronized increases during major global stress episodes, including the late-1990s emerging market crises, the Global Financial Crisis, the euro area sovereign debt crisis, and the COVID-19 shock. While the probability-of-default series displays higher short-term volatility, the close alignment in medium-term movements indicates that Factor 1 captures the common component underlying global banking-sector default risk rather than idiosyncratic fluctuations.

Figure 2: **Loading distributions**

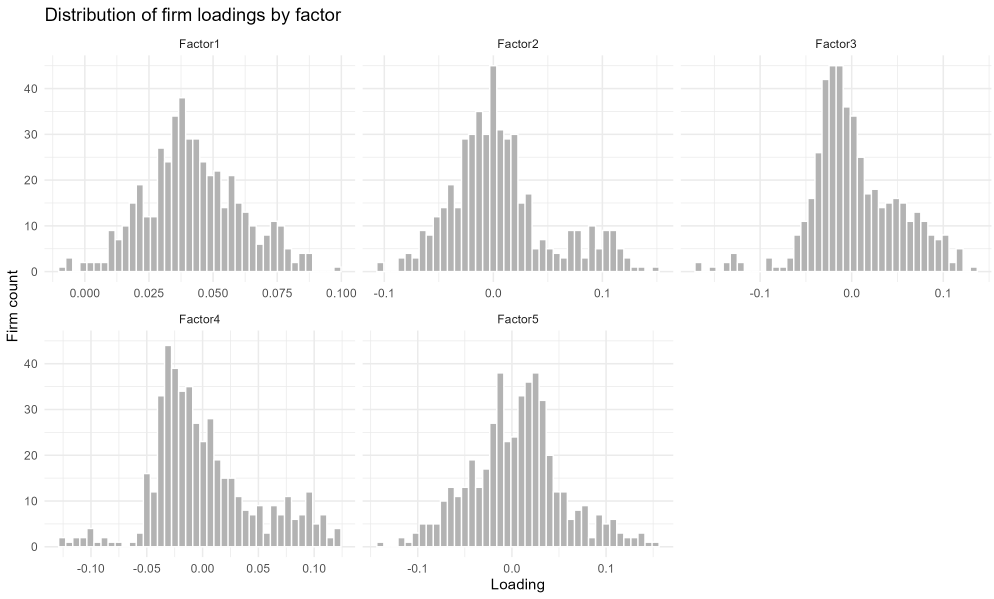

Source: Authors' estimation

Figure 3: **Factor 1, aggregate PD series, and global stress periods**

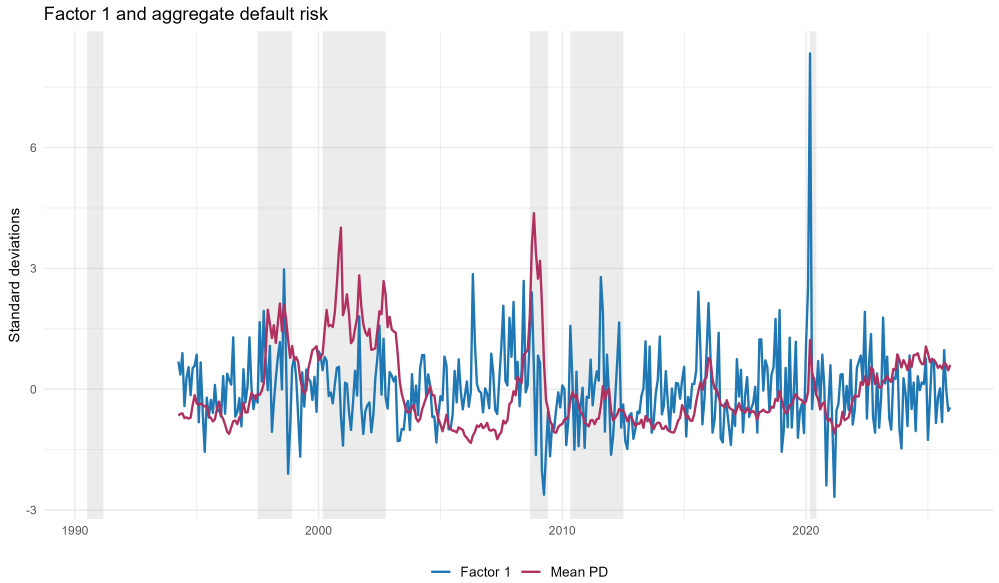

Source: CRI; Authors' estimation

Notes: Both series are standardized (z-scored) prior to plotting to allow visual comparison on a common scale. Factor 1 is a latent variable with no natural units, while the aggregate PD is a probability; expressing both as deviations from their respective means in units of standard deviations makes co-movement patterns directly comparable. Shaded areas denote major global stress episodes.

Figure 3 plots the estimated global default factor alongside the cross-sectional mean PD, both standardized to allow visual comparison. The two series co-move closely across the full sample, consistent with Factor 1 capturing a meaningful common component of aggregate banking-sector stress. Two notable patterns are visible. First, a divergence emerges around 2010: in the pre-2010 period, the aggregate mean PD tends to exceed Factor 1 during stress episodes, whereas post-2010, Factor 1 spikes substantially more than the mean PD. This pattern is consistent with increasing synchronization of banking-sector default risk across firms and countries—if stress has become more globally correlated over time, the common factor would be expected to amplify relative to an equal-weighted average. Second, during the COVID-19 episode, Factor 1 rises approximately five standard deviations above the aggregate mean PD, potentially reflecting the high degree of simultaneity of the shock and the sharp market-implied repricing of bank default risk globally, even as realized defaults remained comparatively contained amid large-scale policy interventions.

The DFM explains approximately 19 percent of within-firm variation in banking-sector default probabilities, with the first factor alone accounting for 11 percent. Subsequent factors each explain substantially smaller shares—on the order of 2 to 3 percent—while higher-order factors contribute only marginally. The concentration of explanatory power in a single dominant factor is consistent with the global banking-sector default cycle documented in Chan-Lau (2026), and is consistent with the view that a single common component accounts for the dominant share of systematic co-movement in bank

default risk across countries.

5.2 Cross-country exposure and synchronization

To assess how banking-sector stress across regions is exposed to the global banking default cycle—and to disentangle the extent to which cross-country co-movement reflects global versus region-specific forces—we proceed in two steps.

First, to assess the extent to which country-level banking-sector stress co-moves with global financial conditions, we examine synchronization between the country banking stress index and the global banking default cycle. Specifically, we compute rolling correlations between country banking stress and the global factor to study how alignment with global banking stress evolves over time.

Second, to evaluate the sources of cross-country co-movement within regions, we compute average within-region pairwise correlations of country banking stress indices. We then repeat this exercise after netting out the global banking default factor from each country's stress index, where the residual is obtained by regressing the country index on the global factor and retaining the residual component. Comparing raw and net-of-global within-region correlations allows us to quantify the extent to which regional co-movement reflects common exposure to global banking stress versus residual regional or domestic factors.

We find that global banking stress acts as a state-dependent force, exerting stronger influence on national banking systems during periods of widespread financial disruption than in normal times. Figure 4[6] shows that synchronization in banking-sector stress intensifies during global financial stress episodes, including the Global Financial Crisis and the COVID-19 shock. This pattern indicates that global banking stress becomes more dominant during periods of widespread financial disruption rather than remaining constant over time.

In particular, several patterns stand out from Figure 4. First, synchronization with the global factor is time-varying rather than constant. Across all regions, correlations are relatively moderate during tranquil periods but rise sharply during episodes of global financial stress. In particular, synchronization increases markedly around the Global Financial Crisis and again during the COVID-19 shock, indicating that global banking-sector stress becomes more dominant precisely when financial conditions deteriorate worldwide. Second, while the increase in synchronization during crises is common across regions, the level and persistence of synchronization differ. Some regions exhibit a sharp but temporary rise that recedes after the crisis (East Asia and Pacific), whereas others display a more sustained elevation in correlation following major global shocks (North America and Latin America). This heterogeneity suggests differences in financial structures, banking-system integration, and exposure to global

[6] Given the high persistence of the underlying series, the rolling correlation estimates should be interpreted with caution, as they may partly reflect shared low-frequency trends rather than time-varying economic relationships.

financial conditions.

We also find the dominant role of the global banking default cycle in shaping cross-country co-movement, while also pointing to meaningful heterogeneity in the strength of residual regional linkages with ASEAN being the one showing the strongest regional linkages. Figure 5 compares average within-region correlations of country banking stress indices computed using raw series with correlations computed after netting out the global banking default factor. The raw correlations are sizable across all regions, suggesting substantial co-movement in banking-sector stress within regions. However, once the global factor is removed, within-region correlations decline sharply in most cases. This finding implies that a large share of apparent regional co-movement reflects common exposure to global banking stress, rather than independent regional dynamics. At the same time, residual correlations remain non-negligible in some regions, such as ASEAN, indicating that regional or domestic factors continue to play a role. These residual co-movements may reflect regional banking integration, common regulatory environments, or shared macroeconomic exposures that are not fully captured by the global factor.

Figure 4: Rolling correlation

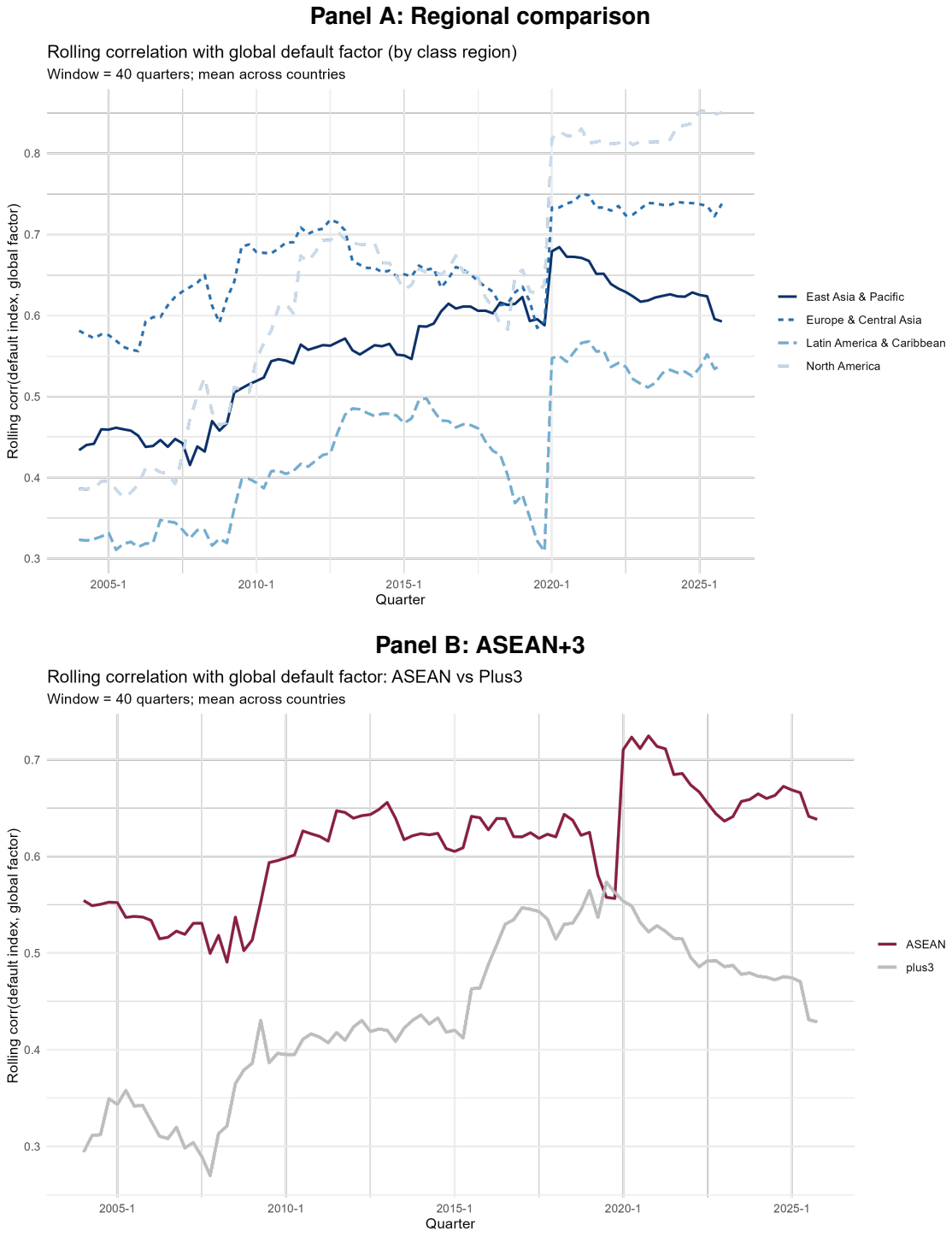

Source: Authors' calculation.

Figure 5: Synchronization within regions

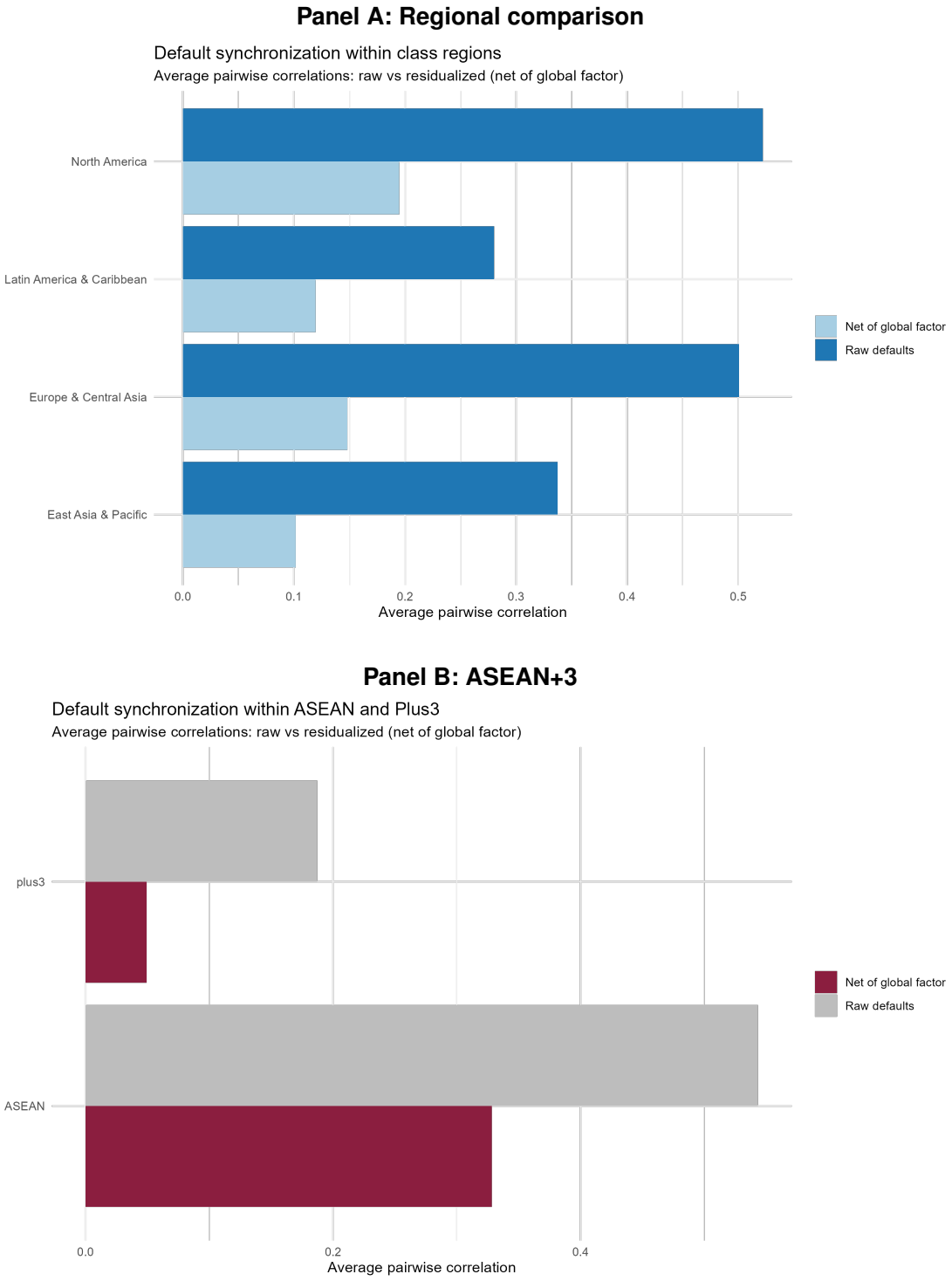

Source: Authors' calculation.

6 Macro-financial linkages of the global banking default cycle

This section examines whether the global banking default cycle contains predictive information for future macro-financial conditions across countries. We study how fluctuations in a global banking-sector stress factor are associated with subsequent movements in output growth and domestic credit conditions using panel local projections. The analysis is designed to focus on the timing, persistence, and state dependence of these associations rather than on structural identification.

Building on the diagnostics in Section 5, we interpret the estimated global factor extracted from banking-sector probabilities of default as a summary measure of common banking-sector stress. By construction, this factor captures the systematic component of market-implied default risk shared across countries and reflects periods in which balance-sheet strains in the banking system become more pronounced. Throughout this section, the local projection estimates are interpreted as predictive dynamic responses that characterize average propagation patterns in the data rather than as structural causal effects.

The empirical analysis proceeds in stages. We first document stylized facts on timing and co-movement between the global banking default cycle and macro-financial variables. We then estimate panel local projections to characterize dynamic responses of GDP growth and credit conditions. Finally, we assess nonlinearities, sample composition effects, and robustness to alternative inference schemes and controls for global risk sentiment.

Figure 6: Lead lag correlations between global banking default factor and macro-financial variables

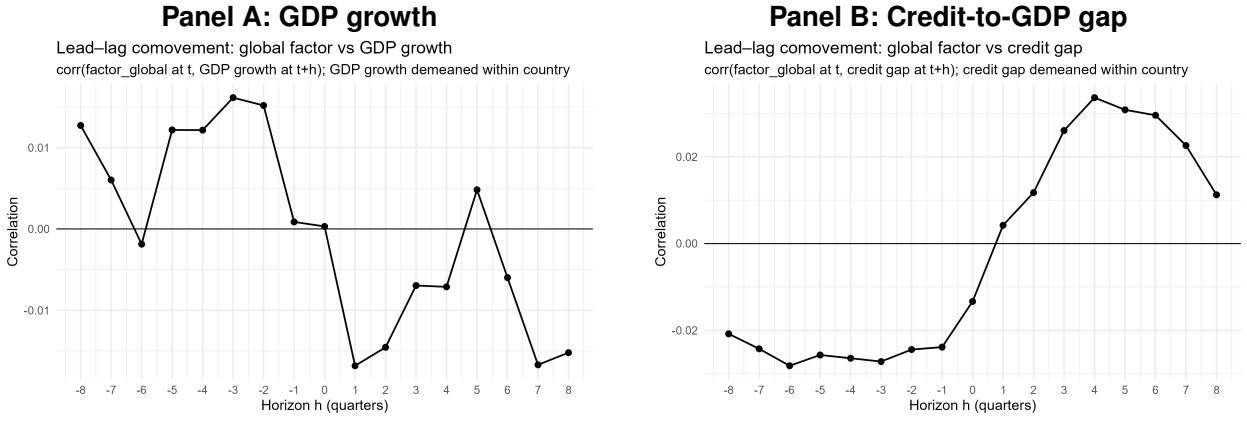

Source: Authors' calculations

Notes: The figure reports unconditional lead lag correlations calculated.

GDP growth and the credit gap both show a degree of co-movement with the global factor, although the lead–lag patterns differ across variables. Figure 6 documents unconditional lead–lag correlations between the global banking default factor and macro-financial indicators. GDP growth exhibits a pro-

nounced negative correlation with the global factor at horizons of one to four quarters, while correlations at negative horizons are small. This pattern indicates that increases in global default stress tend to precede declines in real activity rather than the reverse. In contrast, the credit-to-GDP gap shows strong and persistent co-movement with the global factor, reflecting a close interaction between global banking stress and domestic credit conditions. Elevated global banking-sector default risk typically materializes after periods of credit contraction and is followed by a gradual normalization of credit conditions.

Figure 7: Rolling correlation between global banking default factor and macro-financial variables

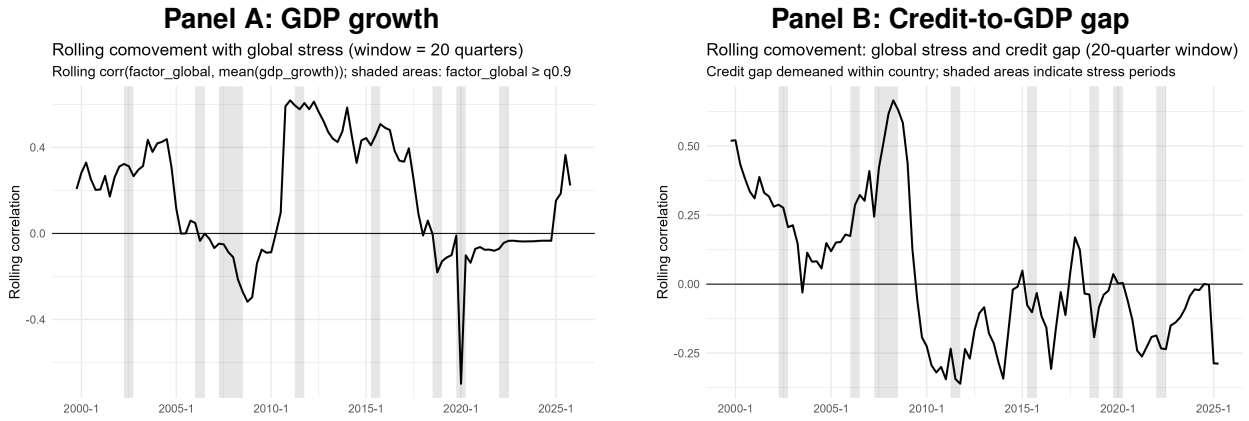

Source: Authors' calculations

Notes: The figure reports 20-quarter rolling contemporaneous correlations between the global banking default factor and macro-financial variables. Shaded regions denote periods of elevated global banking stress (global factor above the 90th percentile).

Rolling correlations between GDP growth and the global banking stress factor indicate a time-varying and potentially nonlinear relationship. Figure 7 shows the rolling contemporaneous correlation between the global banking stress factor and average GDP growth, with shaded regions denoting periods of elevated global stress. Both the magnitude and the sign of the correlation vary substantially over time, with noticeable shifts occurring around stress episodes. This pattern suggests that the association between global banking stress and real activity changes across different phases of the financial cycle rather than remaining constant.

A similarly time-varying relationship is evident between the credit gap and the global banking stress factor. Panel B of Figure 7 presents the 20-quarter rolling contemporaneous correlation between the global banking default factor and the credit-to-GDP gap.[7] The strength and sign of the correlation vary markedly over time, shifting across different phases of the financial cycle. Prior to the global financial crisis, banking stress and credit gaps co-move positively, consistent with periods of credit expansion and rising financial vulnerabilities. In contrast, in the post-crisis period the correlation is predominantly negative, indicating that elevated banking-sector default risk tends to coincide with already-tight credit

[7] The results are robust to alternative window length with similar time-varying patterns observed (see Appendix C).

conditions during phases of balance-sheet repair. This pattern highlights the state-dependent nature of the relationship between banking stress and credit dynamics.

6.1 Baseline results

We find that both real GDP growth and the credit-to-GDP gap are associated with global banking-sector stress, albeit with heterogeneous response timing and magnitude.[8] These results are reported in Table 4, which shows baseline pooled local projection estimates of the dynamic response of GDP growth and the credit-to-GDP gap to a one-standard-deviation increase in the global banking default cycle. The table summarizes horizon-by-horizon coefficients together with pointwise confidence intervals, allowing for a direct comparison of real and financial responses over time.

Figure 8: Baseline local projection impulse responses to global banking stress

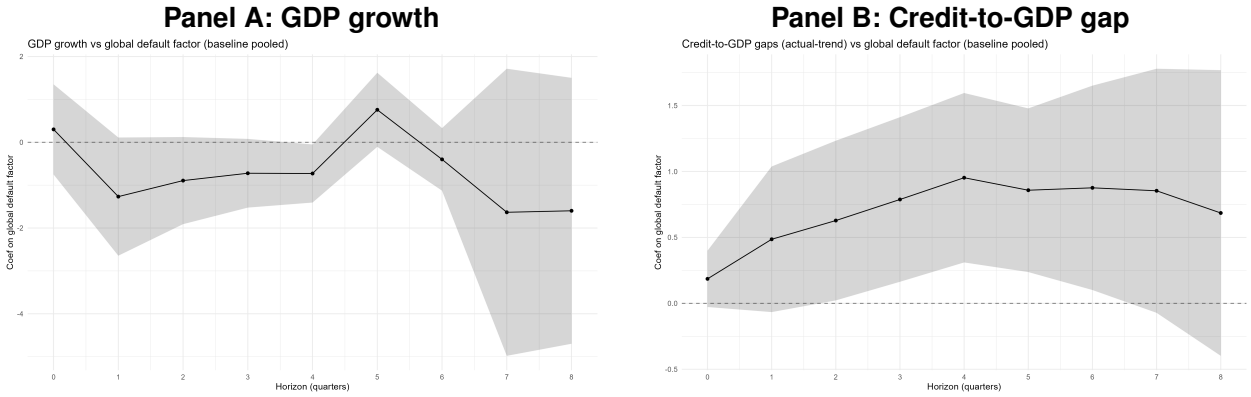

Notes: The figure reports panel local projection estimates of the response of GDP growth (Panel A) and the credit-to-GDP gap (Panel B) to a one-standard-deviation increase in the global banking stress factor G_t. Specifications include country fixed effects. Shaded areas denote 95% pointwise confidence intervals based on country-clustered standard errors.

The estimated response of GDP growth indicates that increases in global banking-sector default risk are followed by declines in real activity with a lag. On impact, the response is small and statistically insignificant, suggesting little contemporaneous adjustment. At a horizon of one quarter, however, a one-standard-deviation increase in the global banking stress factor is associated with a decline in GDP growth of approximately 1.27 percentage points, and the effect is statistically significant at the 10% level at horizons two through three, and at the 5% level at a horizon of four quarters. At the five-quarter horizon, the point estimate reverses sign to approximately 0.76 percentage points, though this result should be interpreted with caution as the underlying impulse response figure indicates wide confidence bands at longer horizons. Beyond five quarters, estimates are statistically insignificant. Taken together,

[8] Results are robust to alternative inference schemes, including two-way clustering by country and quarter, with differences arising only in the width of confidence intervals. Balanced-panel estimates yield smoother and, in some cases, more persistent responses, indicating that baseline unbalanced-panel results are conservative.

the estimates point to a delayed and economically meaningful association between elevated banking-sector stress and subsequent weakness in real activity.

In contrast, the credit-to-GDP gap exhibits a positive and persistent response. Following a one-standard-deviation increase in global banking stress, the credit gap rises by roughly 0.49 percentage points at one quarter and continues to increase over subsequent horizons, reaching nearly one percentage point by one year ahead. The response remains statistically significant over medium horizons before tapering off. This widening of the credit gap should not be interpreted as renewed credit expansion. Rather, it may reflect the relative persistence of credit stocks compared to real activity, as well as denominator effects arising from declines in GDP during stress episodes. In addition, given that credit conditions tend to tighten prior to increases in default stress, the subsequent rise in the gap may partly represent a normalization from previously compressed levels rather than a new phase of credit-driven expansion.[9]

Table 4: Baseline pooled local projections: GDP growth and credit gap

	Estimate	
Horizon	GDP growth	Credit-to-GDP gap
0	0.301	0.186*
1	-1.267*	0.486*
2	-0.894*	0.628**
3	-0.722*	0.788**
4	-0.728**	0.953***
5	0.758*	0.858***
6	-0.399	0.876**
7	-1.633	0.854*
8	-1.598	0.685

Notes: Each horizon h corresponds to a separate local projection relating future macro-financial outcomes to the global banking stress factor. All specifications include country fixed effects. Confidence intervals are pointwise. Significance stars denote *** $p < 0.01$, ** $p < 0.05$, * $p < 0.10$.

[9] Appendix D Figure 15 reports analogous local projections using credit growth as the dependent variable. Credit growth is statistically indistinguishable from zero across horizons in the baseline specification, even as the credit-to-GDP gap widens persistently. This supports interpreting the gap response as reflecting ratio-based adjustment rather than broad-based credit expansion.

6.2 State dependence

Early evidence (Figure 4) shows that country and regional exposure to global banking default cycles can exhibit non-linear and state-dependent features, where higher correlation can be observed during high stress period. To assess nonlinearities, we estimate state-dependent local projections that allow responses to differ between periods of elevated and normal global banking stress. Because the high-stress regime indicator is constructed from the global factor itself, the estimates are descriptive rather than causal: they characterize how the average macro-financial response differs across stress regimes, without identifying the structural source of that variation. Inference focuses on the total high-stress response $\beta_h + \delta_h$, for which we compute 95% confidence intervals derived from the joint variance-covariance matrix of $(\hat{\beta}_h, \hat{\delta}_h)$, which accounts for the covariance between the two components: $\widehat{\mathrm{Var}}(\hat{\beta}_h + \hat{\delta}_h) = \widehat{\mathrm{Var}}(\hat{\beta}_h) + \widehat{\mathrm{Var}}(\hat{\delta}_h) + 2\widehat{\mathrm{Cov}}(\hat{\beta}_h, \hat{\delta}_h)$. We complement the tabular results with impulse response plots that display both regime-specific response paths and their associated confidence bands.

Table 5: State-dependent local projections: GDP growth

	Point estimates			Wald test: $H_0: \beta_h + \delta_h = 0$	
Horizon	Low-stress (β_h)	High–Low (δ_h)	High-stress total $\beta_h + \delta_h$ [95% CI]	Stat.	p-value
0	1.048	-1.321	$-0.272\ [-1.097,\ 0.553]$	0.42	0.518
1	-0.859	-0.721	$-1.580\ [-3.385,\ 0.225]$	2.94	0.086
2	-0.934	0.071	$-0.863\ [-2.161,\ 0.436]$	1.70	0.193
3	0.890	-2.843	$-1.953\ [-3.928,\ 0.022]$	3.76	0.053
4	0.357	-1.907	$-1.550\ [-3.586,\ 0.486]$	2.23	0.136
5	1.918	-2.037	$-0.119\ [-2.862,\ 2.624]$	0.01	0.932
6	0.739	-1.995	$-1.256\ [-3.925,\ 1.414]$	0.85	0.357
7	-2.887	2.198	$-0.689\ [-2.510,\ 1.132]$	0.55	0.458
8	-2.792	2.092	$-0.700\ [-2.603,\ 1.203]$	0.52	0.471

Notes: Each horizon h corresponds to a separate local projection. β_h denotes the response in low-stress periods and δ_h the incremental response in high-stress periods; the total high-stress effect equals $\beta_h + \delta_h$. The 95% confidence interval for the total high-stress response is derived from the joint variance-covariance matrix: $\widehat{\mathrm{Var}}(\hat{\beta}_h + \hat{\delta}_h) = \widehat{\mathrm{Var}}(\hat{\beta}_h) + \widehat{\mathrm{Var}}(\hat{\delta}_h) + 2\widehat{\mathrm{Cov}}(\hat{\beta}_h, \hat{\delta}_h)$. Wald tests assess $H_0: \beta_h + \delta_h = 0$ at each horizon. All confidence intervals are pointwise.

Figure 9: State-dependent impulse responses: GDP growth

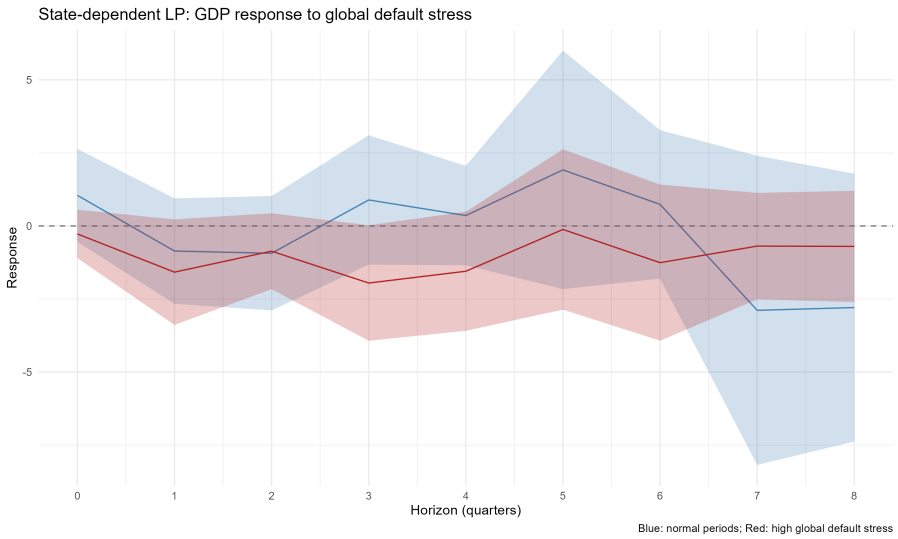

Notes: The figure reports state-dependent local projection impulse responses of GDP growth to a one-standard-deviation increase in the global banking stress factor. Blue shading denotes 95% pointwise confidence intervals for the low-stress regime ($\hat{\beta}_h$); red shading denotes 95% confidence intervals for the total high-stress response ($\hat{\beta}_h + \hat{\delta}_h$), derived from the joint variance-covariance matrix of $(\hat{\beta}_h, \hat{\delta}_h)$. The high-stress regime is defined as periods in which the global factor exceeds its 90th percentile.
Source: Authors' calculations.

Table 5 presents state-dependent local projection estimates for GDP growth. In low-stress periods, the estimated responses $\hat{\beta}_h$ are small and statistically insignificant across all horizons, suggesting limited systematic co-movement between the global default factor and output during tranquil conditions. Under elevated stress—when the global factor exceeds its 90th-percentile threshold—the total estimated response $\hat{\beta}_h + \hat{\delta}_h$ turns negative at most horizons, reaching approximately -1.6 percentage points one quarter ahead. Statistical support for this amplification is limited, with the Wald test attaining marginal significance at the 10% level only at horizons one and three. The estimates are therefore consistent with the association between global banking stress and real activity being concentrated in already stressed environments, though the evidence remains suggestive rather than conclusive.

Table 6 presents analogous estimates for the credit-to-GDP gap. In contrast to the GDP results, the low-stress responses $\hat{\beta}_h$ are positive and accumulate across horizons, indicating that even moderate increases in the global default factor are associated with a widening of the credit gap under tranquil conditions. During high-stress episodes the total response $\hat{\beta}_h + \hat{\delta}_h$ is uniformly positive and larger, peaking at approximately 1.0 percentage point at horizon four. The amplification is most pronounced at short horizons: at $h = 1$ the stress-period increment ($\hat{\delta}_h = 0.44$ pp) exceeds the low-stress response ($\hat{\beta}_h = 0.25$ pp), while at longer horizons the low-stress component dominates and $\hat{\delta}_h$ turns negative. The Wald test rejects the null of no total high-stress effect at the 10% level from horizon one through five, and at the 5% level at horizons three through five, pointing to a statistically meaningful and persistent

widening of credit conditions during episodes of elevated banking stress.

Table 6: State-dependent local projections: Credit-to-GDP gap

	Point estimates			Wald test: $H_0: \beta_h + \delta_h = 0$	
Horizon	Low-stress (β_h)	High–Low (δ_h)	High-stress total $\beta_h + \delta_h$ [95% CI]	Stat.	p-value
0	0.169	0.030	$0.200\ [-0.103,\ 0.503]$	1.67	0.196
1	0.250	0.444	$0.694\ [-0.066,\ 1.454]$	3.21	0.073
2	0.420	0.391	$0.811\ [-0.027,\ 1.650]$	3.60	0.058
3	0.632	0.293	$0.924\ [0.091,\ 1.758]$	4.73	0.030
4	0.864	0.166	$1.030\ [0.208,\ 1.852]$	6.03	0.014
5	1.014	-0.291	$0.722\ [0.059,\ 1.386]$	4.55	0.033
6	1.125	-0.466	$0.659\ [-0.214,\ 1.532]$	2.19	0.139
7	1.336	-0.900	$0.435\ [-0.590,\ 1.461]$	0.69	0.405
8	1.372	-1.283	$0.089\ [-1.074,\ 1.252]$	0.02	0.881

Notes: Each horizon h corresponds to a separate local projection. β_h denotes the response in low-stress periods and δ_h the incremental response in high-stress periods; the total high-stress effect equals $\beta_h + \delta_h$. The 95% confidence interval for the total high-stress response is derived from the joint variance-covariance matrix: $\widehat{\mathrm{Var}}(\hat{\beta}_h + \hat{\delta}_h) = \widehat{\mathrm{Var}}(\hat{\beta}_h) + \widehat{\mathrm{Var}}(\hat{\delta}_h) + 2\widehat{\mathrm{Cov}}(\hat{\beta}_h, \hat{\delta}_h)$. Wald tests assess $H_0 : \beta_h + \delta_h = 0$ at each horizon. All confidence intervals are pointwise.

Figure 10: State-dependent impulse responses: credit-to-GDP gap

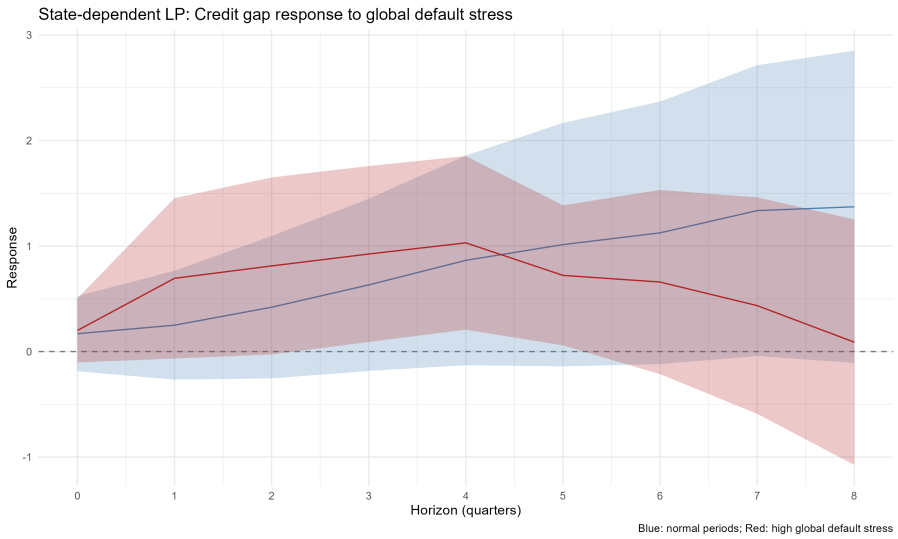

Notes: The figure reports state-dependent local projection impulse responses of the credit-to-GDP gap to a one-standard-deviation increase in the global banking stress factor. Blue shading denotes 95% pointwise confidence intervals for the low-stress regime ($\hat{\beta}_h$); red shading denotes 95% confidence intervals for the total high-stress response ($\hat{\beta}_h + \hat{\delta}_h$), derived from the joint variance-covariance matrix of $(\hat{\beta}_h, \hat{\delta}_h)$. The high-stress regime is defined as periods in which the global factor exceeds its 90th percentile.
Source: Authors' calculations.

6.3 Robustness

Incremental information relative to the VIX. A natural concern is whether the global banking default factor captures distinct macro-financial information or largely proxies for conventional measures of global risk sentiment. To assess this, we augment the baseline specification with the log VIX (standardized), which serves as a widely used benchmark for global risk appetite:

$$y_{c,t+h} = \alpha_c + \beta_h G_t + \phi_h \mathrm{VIX}_t + \Gamma_h X_{c,t} + \varepsilon_{c,t+h}. \tag{14}$$

Table 7 reports the results. Two findings stand out. First, for GDP growth, controlling for the VIX substantially attenuates the estimated coefficient on the global default factor, which loses statistical significance at most horizons. This indicates that the predictive content of global banking stress for output growth overlaps considerably with that of the VIX, reflecting the close co-movement between market-implied default risk and broader risk sentiment during stress episodes. We therefore interpret the baseline GDP estimates as an upper bound on the incremental contribution of the default factor beyond standard risk proxies.

Second, for the credit-to-GDP gap, the global default factor retains marginal significance at horizons three through five quarters after conditioning on the VIX, with coefficients broadly comparable to the baseline. Significance at shorter horizons—one and two quarters—is not maintained, suggesting that the early credit gap response overlaps with the information already captured by the VIX. The VIX coefficients for credit are negative throughout but statistically insignificant, which is consistent with the default factor capturing a dimension of banking-sector stress not fully reflected in aggregate volatility measures, though the evidence remains marginal.

Table 7: Baseline pooled LP with VIX control: GDP growth and credit-to-GDP gap

	GDP growth		Credit-to-GDP gap	
Horizon	Global factor [CI]	VIX [CI]	Global factor [CI]	VIX [CI]
0	$0.852\ [-0.586,\ 2.290]$	$-2.256^{*}\ [-4.947,\ 0.436]$	$0.352\ [-0.231,\ 0.934]$	$-0.427\ [-1.717,\ 0.863]$
1	$-1.147^{*}\ [-2.507,\ 0.212]$	$-1.435\ [-3.615,\ 0.744]$	$0.605\ [-0.218,\ 1.428]$	$-0.384\ [-1.817,\ 1.048]$
2	$-0.655\ [-1.530,\ 0.220]$	$-1.829\ [-4.818,\ 1.159]$	$0.701\ [-0.189,\ 1.591]$	$-0.432\ [-1.921,\ 1.056]$
3	$0.117\ [-1.193,\ 1.426]$	$-3.536\ [-9.572,\ 2.500]$	$0.812^{*}\ [-0.145,\ 1.768]$	$-0.473\ [-2.178,\ 1.232]$
4	$-0.149\ [-1.164,\ 0.865]$	$-2.309\ [-7.666,\ 3.048]$	$0.979^{*}\ [-0.006,\ 1.963]$	$-0.689\ [-2.462,\ 1.085]$
5	$1.749\ [-1.025,\ 4.524]$	$-2.615\ [-8.795,\ 3.564]$	$0.870^{*}\ [-0.079,\ 1.820]$	$-0.886\ [-2.690,\ 0.918]$
6	$0.647\ [-1.076,\ 2.370]$	$-2.242\ [-6.589,\ 2.106]$	$0.795\ [-0.229,\ 1.820]$	$-0.852\ [-2.702,\ 0.998]$
7	$-0.606\ [-2.335,\ 1.122]$	$-1.514\ [-5.158,\ 2.130]$	$0.811\ [-0.359,\ 1.980]$	$-1.151\ [-3.063,\ 0.762]$
8	$-0.406\ [-1.784,\ 0.973]$	$-1.254\ [-4.005,\ 1.497]$	$0.700\ [-0.609,\ 2.010]$	$-1.440\ [-3.440,\ 0.560]$

Notes: Each horizon h corresponds to a separate local projection including both the global banking default factor and the log VIX (standardized) as regressors. All specifications include country fixed effects. Confidence intervals are pointwise based on two-way clustered standard errors. Significance stars: $^{***}\ p < 0.01$, $^{**}\ p < 0.05$, $^{*}\ p < 0.10$.

Reverse causality: lead test. To assess whether the baseline estimates reflect genuine predictive content of global banking stress or are contaminated by reverse causality—whereby deteriorating macro conditions feed back into future default risk—we augment the baseline specification with one-quarter-ahead leads of the global factor. Specifically, we estimate:

$$y_{c,t+h} = \alpha_c + \beta_h G_t + \gamma_h G_{t+1} + \Gamma_h X_{c,t} + \varepsilon_{c,t+h}, \tag{15}$$

where G_{t+1} is included alongside the contemporaneous factor G_t. The key diagnostic logic is that future realizations of the global factor should not add predictive power for current macro outcomes once the contemporaneous factor is controlled for. If G_{t+1} is significant, this would raise concerns that the baseline estimates partly reflect reverse prediction or common omitted dynamics. A statistically significant $\hat{\gamma}_h$ would indicate either that macro conditions predict subsequent banking stress (reverse causality) or that a common unobserved shock is driving both series.

Figures 11 and 12 report the estimated $\hat{\gamma}_h$ coefficients across horizons for GDP growth and the credit

gap, respectively.

For GDP growth (Figure 11), the coefficient on G_{t+1} is statistically indistinguishable from zero at most horizons, with a marginally significant result appearing at horizon six. At the short to medium horizons where the baseline GDP responses are most pronounced, the lead coefficient is not significant, which is broadly consistent with limited reverse causality at those horizons. The result at horizon six introduces some uncertainty at longer horizons and should be interpreted with caution.

For the credit gap (Figure 12), the coefficient on G_{t+1} is positive at medium horizons but remains statistically insignificant throughout. The positive direction is consistent with an anticipation channel—credit conditions may tighten ahead of the realization of balance-sheet stress—but the absence of statistical significance means we cannot reject the null of no reverse causality. Together, these results support interpreting the baseline LP estimates as reflecting predictive associations running from global banking stress to macro-financial outcomes rather than the reverse.

Figure 11: Lead test: coefficient on G_{t+1} in GDP growth LP

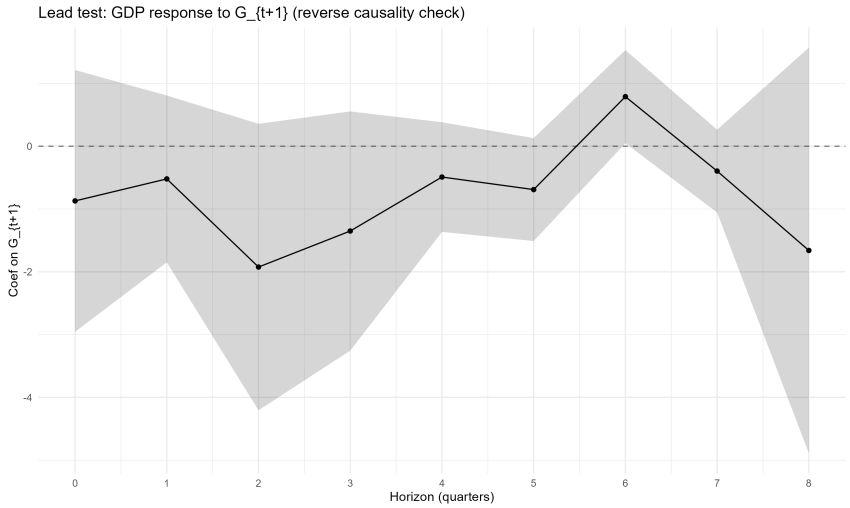

Notes: The figure reports the coefficient $\hat{\gamma}_h$ on G_{t+1} from equation (15), which includes both G_t and G_{t+1} as regressors. Under no reverse causality, $\hat{\gamma}_h$ should be zero at all horizons. Shaded areas denote 95% pointwise confidence intervals based on two-way clustered standard errors.
Source: Authors' calculations.

Figure 12: Lead test: coefficient on G_{t+1} in credit gap LP

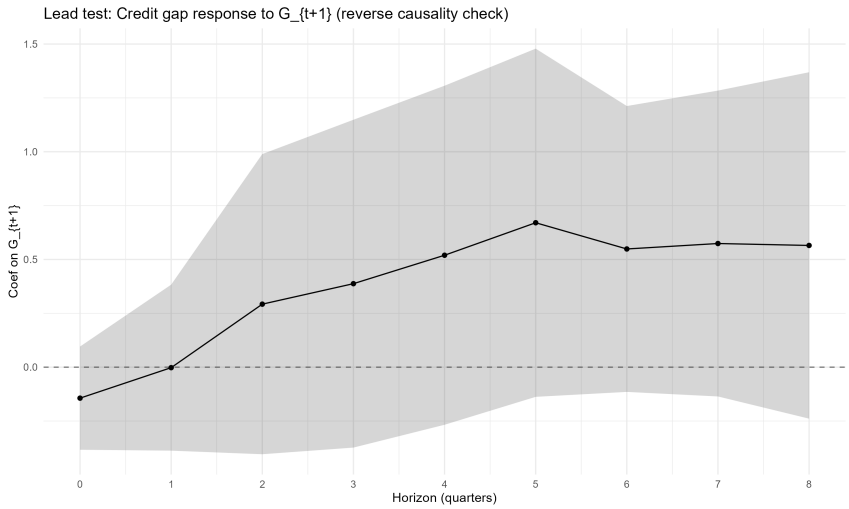

Notes: The figure reports the coefficient $\hat{\gamma}_h$ on G_{t+1} from equation (15) for the credit gap specification. The positive but insignificant direction at medium horizons is consistent with an anticipation channel but does not constitute evidence of reverse causality. Shaded areas denote 95% pointwise confidence intervals based on two-way clustered standard errors. *Source:* Authors' calculations.

7 Conclusion

This paper studies the global banking default cycle and its macro-financial implications using market-implied measures of bank default risk. We construct a global banking stress factor from firm-level default probabilities and derive country-level banking stress indices based on dynamic factor model–imputed series. This approach allows us to isolate common movements in banking-sector default risk while mitigating the effects of missing observations and idiosyncratic firm-level noise.

Our analysis documents a high degree of synchronization in banking-sector stress across countries, with co-movement rising markedly during periods of elevated global stress. Rolling correlation evidence shows that country-level banking stress indices align more closely with the global factor during stress episodes, while within-region co-movement persists in some regions—notably ASEAN—even after netting out the global component, though correlations decline sharply in most cases. These patterns indicate that global banking stress is a central force shaping cross-country dynamics in bank default risk, particularly during stress episodes.

We then assess the macro-financial linkages of the global banking default cycle using panel local projections. Baseline estimates show that increases in global banking stress are followed by a delayed decline in real economic activity and a persistent widening of credit gaps. The GDP growth responses materialize at medium horizons, consistent with gradual propagation through financial intermediation

rather than immediate demand channels. By contrast, credit-to-GDP gaps tend to rise following increases in global banking stress, reflecting the heterogeneous adjustment of credit stocks and real activity during stress episodes.

Allowing for nonlinearities reveals suggestive evidence of state dependence in these average responses. When global banking stress is elevated—defined as periods in which the global factor exceeds its 90th percentile—the contractionary association with GDP growth becomes economically larger and is marginally statistically significant at selected horizons, while responses during normal periods are muted. For credit conditions, stress episodes are associated with a pronounced and persistent widening of credit gaps, whereas effects outside high-stress regimes are weaker and less precisely estimated. Wald tests provide statistical support for the total high-stress response at several horizons, with more consistent evidence for credit conditions than for GDP growth, pointing to the role of global banking stress as an amplifier of credit dynamics during periods of synchronized financial tightening. Robustness checks, including alternative inference schemes, a VIX control, lead–lag specifications, and balanced panel estimates, support the main conclusions.

The results indicate that the global banking default cycle is systematically associated with macro-financial outcomes and that these associations vary across stress regimes. Increases in global banking-sector default risk are followed by declines in real activity, particularly during periods of elevated stress, while credit dynamics exhibit more persistent adjustment patterns. These findings suggest that market-implied banking-sector default risk captures a dimension of global financial conditions that is not fully reflected in traditional indicators of volatility or credit aggregates, particularly for credit dynamics. In this sense, the global default factor summarizes periods in which underlying vulnerabilities are reflected in market-based measures of banking stress. Monitoring developments in global banking stress may therefore provide useful information about evolving macro-financial conditions, especially in environments characterized by synchronized financial strain.

From a policy perspective, these findings suggest that market-implied banking-sector default risk can complement traditional macro-financial indicators by highlighting periods in which underlying vulnerabilities become more salient for real economic outcomes. The distinction between vulnerability buildup and stress realization may be particularly relevant for surveillance frameworks that rely heavily on credit-based measures. Moreover, the state-dependent nature of the associations documented here implies that the macroeconomic relevance of financial stress increases once stress is already elevated, underscoring the value of monitoring global banking conditions alongside domestic indicators.

References

Adrian, T. and Shin, H. S. (2010). Liquidity and leverage. *Journal of Financial Intermediation*, 19(3):418–437.

Bai, J. and Ng, S. (2002). Determining the number of factors in approximate factor models. *Econometrica*, 70(1):191–221.

Bai, J. and Ng, S. (2008). Large dimensional factor analysis. *Foundations and Trends in Econometrics*, 3(2):89–163.

Bernanke, B. S., Gertler, M., and Gilchrist, S. (1999). The financial accelerator in a quantitative business cycle framework. *Handbook of Macroeconomics*, 1:1341–1393.

Chamberlain, G. and Rothschild, M. (1983). Arbitrage, factor structure, and mean-variance analysis on large asset markets. *Econometrica*, 51(5):1281–1304.

Chan-Lau, J. A. (2026). Banking and industrial default cycles: Dynamics, spillovers and macroprudential implications. Working Paper 6075883, SSRN. Available at SSRN.

CRI, C. R. I. (2023). Nus credit research initiative technical report. Technical report, National University of Singapore.

Doz, C., Giannone, D., and Reichlin, L. (2012). A quasi—maximum likelihood approach for large, approximate dynamic factor models. *The Review of Economics and Statistics*, 94(4):1014–1024.

Duan, J.-C. and Fulop, A. (2013). Multiperiod corporate default prediction with the partially-conditioned forward intensity. *Available at SSRN 2151174*.

Duan, J.-C., Sun, J., and Wang, T. (2012). Multiperiod corporate default prediction—a forward intensity approach. *Journal of Econometrics*, 170(1):191–209.

Duffie, D., Eckner, A., Horel, G., and Saita, L. (2009). Frailty correlated default. *The Journal of Finance*, 64(5):2089–2123.

Geweke, J. (1977). The dynamic factor analysis of economic time series. *Latent Variables in Socio-Economic Models*, pages 365–383.

Giannone, D., Reichlin, L., and Sala, L. (2004). Monetary policy in real time. In Gertler, M. and Rogoff, K., editors, *NBER Macroeconomics Annual*, volume 19, pages 161–200. University of Chicago Press, Chicago.

Gilchrist, S. and Zakrajšek, E. (2012). Credit spreads and business cycle fluctuations. *American Economic Review*, 102(4):1692–1720.

Jordà, Ò. (2005). Estimation and inference of impulse responses by local projections. *American Economic Review*, 95(1):161–182.

Jordà, O., Singh, S. R., and Taylor, A. M. (2024). The long-run effects of monetary policy. Working Paper 2020-01, Federal Reserve Bank of San Francisco.

Kiyotaki, N. and Moore, J. (1997). Credit cycles. *Journal of Political Economy*, 105(2):211–248.

Koopman, S. J. and Lucas, A. (2005). Business and default cycles for credit risk. *Journal of Applied Econometrics*, 20(2):311–323.

López-Salido, D., Stein, J. C., and Zakrajšek, E. (2017). Credit-market sentiment and the business cycle. *The Quarterly Journal of Economics*, 132(3):1373–1426.

Miranda-Agrippino, S. and Rey, H. (2020). Us monetary policy and the global financial cycle. *Review of Economic Studies*, 87(6):2754–2776.

Montiel Olea, J. L., Plagborg-Møller, M., Qian, E., and Wolf, C. K. (2024). Double robustness of local projections and some unpleasant varithmetic. Working Paper 32495, National Bureau of Economic Research.

Quah, D. and Sargent, T. J. (1993). A dynamic index model for large cross sections.

Rey, H. (2015). Dilemma not trilemma: The global financial cycle and monetary policy independence. *NBER Working Papers*, (21162).

Sargent, T. J. (1989). Two models of measurement and the investment accelerator. *Journal of Political Economy*, 97(2):251–287.

Shin, H. S. (2013). The second phase of global liquidity and its impact on emerging economies. *Global Liquidity, Federal Reserve Bank of Kansas City*.

Stock, J. H. and Watson, M. W. (1989). New indexes of coincident and leading economic indicators. In Blanchard, O. J. and Fischer, S., editors, *NBER Macroeconomics Annual*, volume 4, pages 351–394. MIT Press, Cambridge, MA.

Stock, J. H. and Watson, M. W. (2002). Forecasting using principal components from a large number of predictors. *Journal of the American Statistical Association*, 97(460):1167–1179.

Stock, J. H. and Watson, M. W. (2011). Dynamic factor models. In *The Oxford Handbook of Economic Forecasting*. Oxford University Press.

Appendix

A Robustness to the Number of Factors

To assess the sensitivity of the estimated global banking default factor to the choice of factor dimension, the dynamic factor model is re-estimated using alternative numbers of latent factors. Figure 13 compares the resulting estimates of the dominant factor across specifications. The results show that the global factor is highly stable across alternative choices of the factor dimension, with nearly identical time-series dynamics and closely aligned peaks during major stress episodes. Pairwise correlations between the baseline factor and alternative specifications exceed 0.999. This indicates that the identification of the global banking default cycle is not sensitive to the specific number of factors used in the baseline specification.[10]

Figure 13: Global default factor: sensitivity to the number of factors

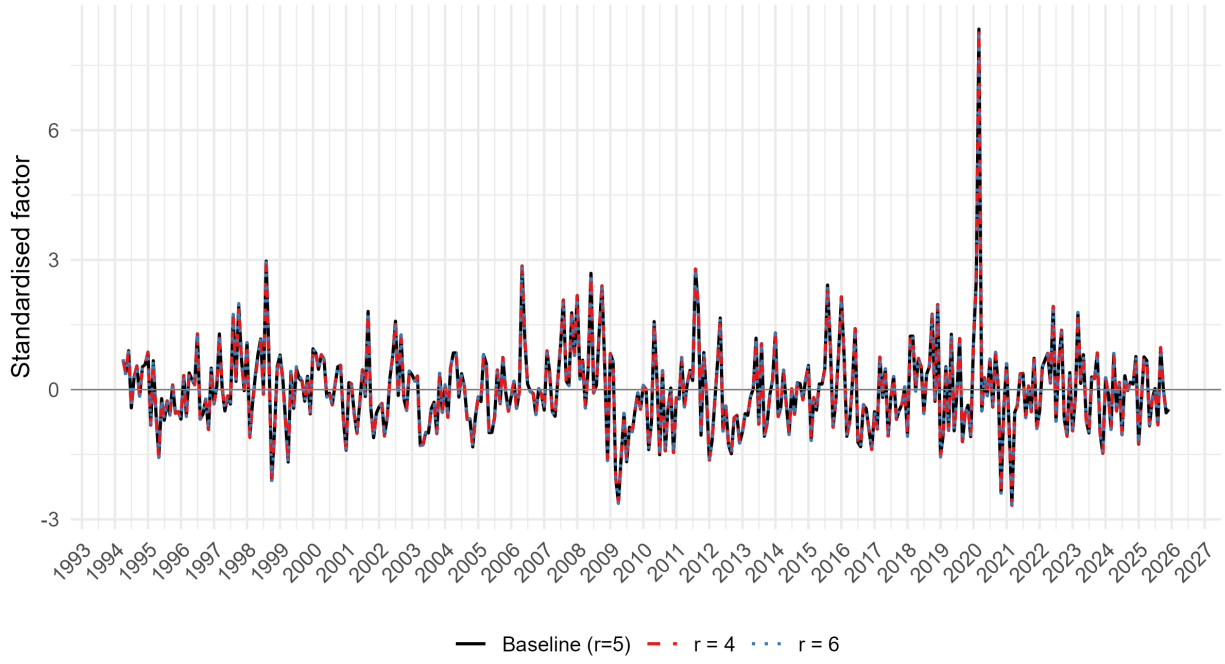

Note: Standardized first factor.

Source: Author's estimations

[10] For computational efficiency, this robustness exercise uses the DGR estimator. The baseline results are based on the BM approach, but results are qualitatively unchanged across estimation methods.

Table 8: Pairwise correlations of standardized global factor across DFM specification

Specification	Baseline	r = 4	r = 6
Baseline	1.0000	0.9999	0.9999
r = 4	0.9999	1.0000	0.9998
r = 6	0.9999	0.9998	1.0000

Source: Author's estimations

B Summary Statistics

Table 9: Summary Statistics

Variable	Mean	Median	Std. Dev.	Minimum	Maximum
Factor 1	0.009	-0.551	7.277	-19.450	60.686
Factor 2	0.298	-0.042	4.171	-18.376	22.281
Factor 3	-0.283	-0.136	3.626	-16.581	12.581
Factor 4	-0.104	-0.134	3.917	-14.117	11.580
Factor 5	-0.187	-0.002	2.325	-16.508	5.749

Source: Author's estimations

C Robustness to Rolling Window Length

To assess the sensitivity of the rolling correlation results to the choice of window length, we recompute the correlations using 12-, 16-, and 24-quarter windows. As shown in Figure 14, the main qualitative patterns remain unchanged across specifications. Shorter windows yield more volatile estimates, reflecting the persistence of the underlying series, and should therefore be interpreted with some caution. Overall, the results indicate that the documented time-varying relationship between global banking stress and credit conditions is not driven by the specific choice of a 20-quarter window.

Figure 14: Rolling correlations between global banking default factor and credit-to-GDP gap under alternative window lengths

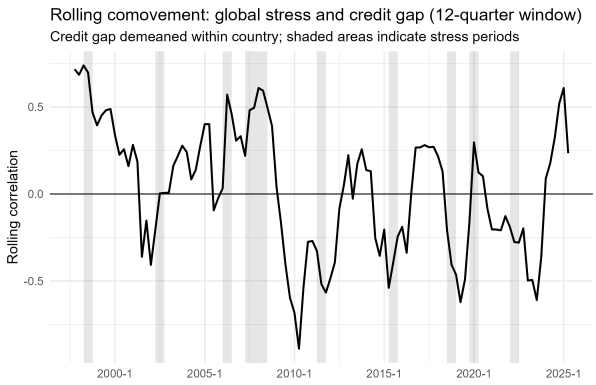

(a) 12-quarter window

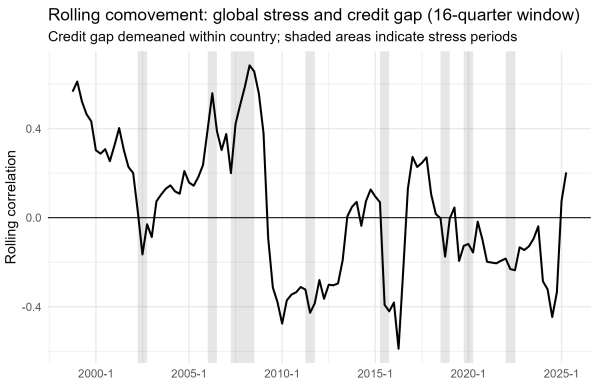

(b) 16-quarter window

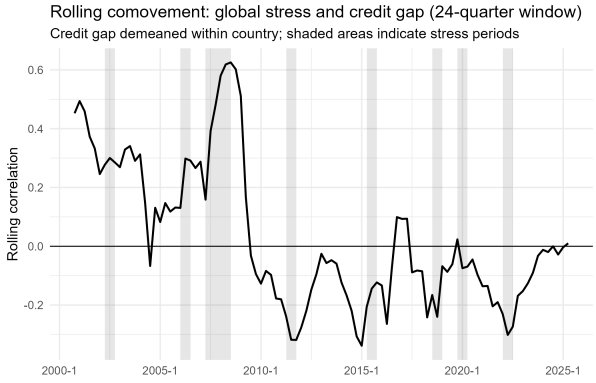

(c) 20-quarter window (baseline)

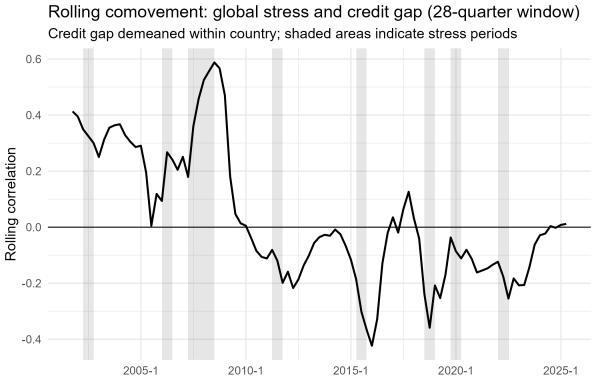

(d) 24-quarter window

Notes: Each panel reports rolling contemporaneous correlations using the indicated window length. Shorter windows yield more volatile estimates, while longer windows smooth high-frequency variation. The main time-varying patterns are robust across specifications.
Source: Author's estimation

D Credit Growth Response

Figure 15: Credit growth impulse responses to global banking stress

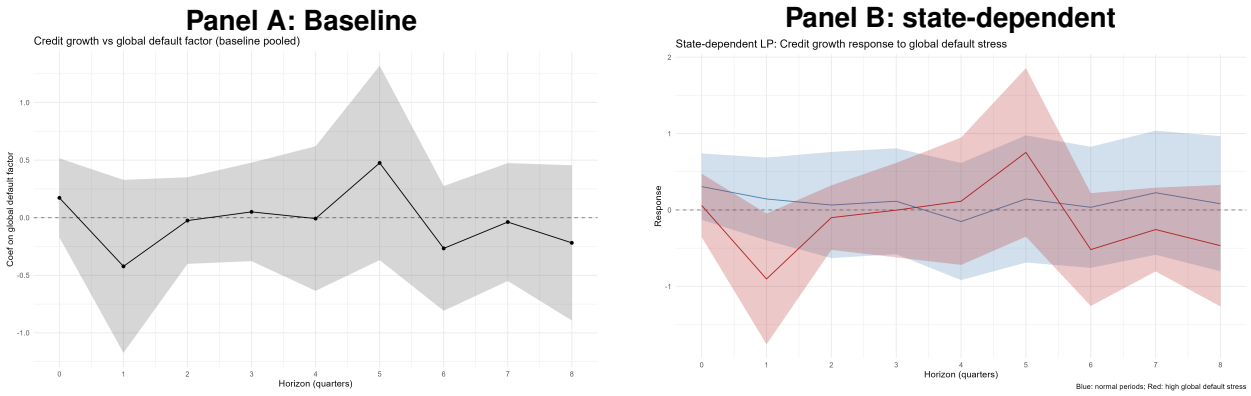

Notes: The figure reports panel local projection estimates of the response of credit growth to a one-standard-deviation increase in the global banking stress factor. Panel A reports the baseline pooled specification, while Panel B reports the state-dependent specification. Specifications include country fixed effects. Shaded areas denote 95% pointwise confidence intervals based on country-clustered standard errors. In Panel B, blue denotes normal periods and red denotes high-stress periods.

E Robustness to Stress Regime Threshold

The high-stress regime indicator in the baseline is defined using the 90th percentile of the global banking default factor. Tables 10 and 11 report full state-dependent local projection results under the 85th percentile threshold; Tables 12 and 13 report the corresponding results under the 95th percentile, to be compared with the baseline 90th percentile results in Tables 5 and 6 in the main text.

Across all three thresholds, the qualitative pattern is consistent: the total high-stress GDP response is negative at medium horizons and the total high-stress credit gap response is positive, with effects concentrating between one and five quarters ahead. For the credit-to-GDP gap, estimated magnitudes at peak horizons tend to increase with the percentile cutoff, consistent with larger macro-financial effects during more extreme stress episodes. For GDP growth, the 85th percentile specification yields stronger statistical precision due to the larger high-stress sample, while the 95th percentile produces less precisely estimated responses given fewer qualifying observations. Overall, the main conclusions from the baseline are robust to the choice of threshold.

Table 10: State-dependent local projections: GDP growth — 85th percentile threshold

Horizon	Low-stress β_h [95% CI]	High–Low δ_h [95% CI]	High-stress total $\beta_h + \delta_h$ [95% CI]	Wald stat.	p-value
0	1.360 [-0.830, 3.551]	-1.717 [-4.340, 0.907]	-0.356 [-1.137, 0.425]	0.80	0.372
1	-0.862 [-2.739, 1.016]	-0.656 [-3.416, 2.103]	-1.518 [-3.302, 0.266]	2.78	0.095
2	-0.905 [-2.884, 1.073]	0.019 [-2.384, 2.421]	-0.887 [-2.083, 0.310]	2.11	0.146
3	0.043 [-1.154, 1.241]	-1.238 [-2.992, 0.515]	-1.195 [-2.083, -0.307]	6.96	0.008
4	-0.591 [-1.801, 0.620]	-0.222 [-1.316, 0.872]	-0.813 [-1.335, -0.290]	9.28	0.002
5	1.317 [-1.483, 4.116]	-0.900 [-4.695, 2.896]	0.417 [-1.052, 1.886]	0.31	0.578
6	-0.131 [-1.269, 1.007]	-0.430 [-2.298, 1.438]	-0.562 [-1.757, 0.634]	0.85	0.357
7	-3.212 [-9.177, 2.752]	2.539 [-2.101, 7.179]	-0.673 [-2.413, 1.066]	0.58	0.448
8	-3.138 [-8.086, 1.810]	2.474 [-0.984, 5.931]	-0.664 [-2.613, 1.285]	0.45	0.504

Notes: Each horizon h corresponds to a separate local projection. β_h denotes the response in low-stress periods and δ_h the incremental response in high-stress periods; the total high-stress effect equals $\beta_h + \delta_h$. Confidence intervals in brackets are 95% pointwise intervals derived from the joint variance-covariance matrix: $\widehat{\mathrm{Var}}(\hat{\beta}_h + \hat{\delta}_h) = \widehat{\mathrm{Var}}(\hat{\beta}_h) + \widehat{\mathrm{Var}}(\hat{\delta}_h) + 2\widehat{\mathrm{Cov}}(\hat{\beta}_h, \hat{\delta}_h)$. Wald tests assess $H_0 : \beta_h + \delta_h = 0$ at each horizon. All specifications include country fixed effects.

Table 11: State-dependent local projections: credit-to-GDP gap — 85th percentile threshold

Horizon	Low-stress β_h [95% CI]	High–Low δ_h [95% CI]	High-stress total $\beta_h + \delta_h$ [95% CI]	Wald stat.	p-value
0	0.156 [-0.275, 0.586]	0.050 [-0.540, 0.641]	0.206 [-0.079, 0.492]	2.01	0.157
1	0.237 [-0.385, 0.860]	0.421 [-0.663, 1.504]	0.658 [-0.091, 1.408]	2.96	0.085
2	0.361 [-0.448, 1.169]	0.453 [-0.798, 1.704]	0.814 [0.023, 1.604]	4.07	0.044
3	0.644 [-0.351, 1.639]	0.243 [-1.182, 1.667]	0.887 [0.054, 1.719]	4.35	0.037
4	0.878 [-0.300, 2.056]	0.126 [-1.443, 1.696]	1.004 [0.181, 1.827]	5.72	0.017
5	1.054 [-0.297, 2.406]	-0.331 [-1.984, 1.322]	0.724 [0.036, 1.411]	4.25	0.039
6	1.195 [-0.233, 2.622]	-0.537 [-2.334, 1.260]	0.658 [-0.221, 1.537]	2.15	0.142
7	1.400 [-0.161, 2.960]	-0.917 [-2.952, 1.117]	0.482 [-0.561, 1.525]	0.82	0.365
8	1.453 [-0.242, 3.148]	-1.290 [-3.521, 0.940]	0.163 [-1.020, 1.345]	0.07	0.788

Notes: See notes to Table 10.

Table 12: State-dependent local projections: GDP growth — 95th percentile threshold

Horizon	Low-stress β_h [95% CI]	High–Low δ_h [95% CI]	High-stress total $\beta_h + \delta_h$ [95% CI]	Wald stat.	p-value
0	0.805 [-0.155, 1.765]	-1.089 [-2.271, 0.092]	-0.284 [-1.284, 0.715]	0.31	0.577
1	-0.882 [-2.697, 0.933]	-0.831 [-4.022, 2.360]	-1.713 [-3.800, 0.373]	2.59	0.108
2	-1.100 [-3.211, 1.011]	0.445 [-3.135, 4.025]	-0.655 [-2.745, 1.435]	0.38	0.539
3	-0.002 [-1.014, 1.011]	-1.554 [-3.514, 0.407]	-1.555 [-2.723, -0.387]	6.81	0.009
4	-0.559 [-1.504, 0.385]	-0.364 [-1.791, 1.063]	-0.923 [-1.929, 0.084]	3.23	0.072
5	0.662 [-1.785, 3.110]	0.205 [-3.702, 4.111]	0.867 [-0.772, 2.507]	1.07	0.300
6	-0.640 [-2.474, 1.193]	0.517 [-2.750, 3.784]	-0.123 [-1.781, 1.535]	0.02	0.884
7	-3.006 [-7.707, 1.694]	2.941 [-0.300, 6.182]	-0.065 [-1.510, 1.380]	0.01	0.930
8	-2.854 [-7.209, 1.502]	2.688 [-0.281, 5.656]	-0.166 [-1.543, 1.211]	0.06	0.813

Notes: See notes to Table 10.

Table 13: State-dependent local projections: credit-to-GDP gap — 95th percentile threshold

Horizon	Low-stress β_h [95% CI]	High–Low δ_h [95% CI]	High-stress total $\beta_h + \delta_h$ [95% CI]	Wald stat.	p-value
0	0.127 [-0.166, 0.419]	0.139 [-0.297, 0.575]	0.265 [-0.002, 0.533]	3.79	0.052
1	0.192 [-0.256, 0.639]	0.692 [-0.168, 1.551]	0.883 [0.202, 1.565]	6.45	0.011
2	0.330 [-0.279, 0.939]	0.701 [-0.317, 1.718]	1.031 [0.303, 1.758]	7.71	0.005
3	0.557 [-0.208, 1.321]	0.541 [-0.575, 1.656]	1.098 [0.362, 1.833]	8.56	0.003
4	0.798 [-0.115, 1.711]	0.362 [-0.870, 1.595]	1.160 [0.426, 1.895]	9.58	0.002
5	1.054 [-0.004, 2.112]	-0.459 [-1.754, 0.837]	0.596 [0.006, 1.185]	3.92	0.048
6	1.340 [0.167, 2.514]	-1.085 [-2.481, 0.310]	0.255 [-0.344, 0.854]	0.70	0.404
7	1.500 [0.237, 2.763]	-1.506 [-3.042, 0.029]	-0.006 [-0.670, 0.658]	0.00	0.986
8	1.492 [0.132, 2.852]	-1.880 [-3.560, -0.200]	-0.388 [-1.163, 0.388]	0.96	0.327

Notes: See notes to Table 10.

Address: 10 Shenton Way, #15-08
MAS Building, Singapore 079117
Website: www.amro-asia.org
Tel: +65 6323 9844
Email: enquiry@amro-asia.org
LinkedIn | **Twitter** | **Facebook**